

A Novel Approach to the Initial Value Problem with a Complete Validated Algorithm [★]

Bingwei Zhang^{a,1}, Chee Yap^{a,*}

^aThe Courant Institute of Mathematical Sciences, Department of Computer Science, New York, NY 10012, USA

ARTICLE INFO

Keywords:

initial value problem, IVP, reachability problem, enclosure problem, radical transform, validated algorithms, interval methods, logarithmic norm, matrix measure, contraction maps

ABSTRACT

We consider the first order autonomous differential equation (ODE) $\mathbf{x}' = \mathbf{f}(\mathbf{x})$ where $\mathbf{f} : \mathbb{R}^n \rightarrow \mathbb{R}^n$ is locally Lipschitz. For $\mathbf{x}_0 \in \mathbb{R}^n$ and $h > 0$, the initial value problem (IVP) for $(\mathbf{f}, \mathbf{x}_0, h)$ is to determine if there is a unique solution, i.e., a function $\mathbf{x} : [0, h] \rightarrow \mathbb{R}^n$ that satisfies the ODE with $\mathbf{x}(0) = \mathbf{x}_0$. Write $\mathbf{x} = \text{IVP}_{\mathbf{f}}(\mathbf{x}_0, h)$ for this unique solution.

We pose a corresponding computational problem, called the **End Enclosure Problem**: given $(\mathbf{f}, B_0, h, \varepsilon_0)$ where $B_0 \subseteq \mathbb{R}^n$ is a box and $\varepsilon_0 > 0$, to compute a pair of non-empty boxes (B_0, B_1) such that $B_0 \subseteq B_1$, width of B_1 is $< \varepsilon_0$, and for all $\mathbf{x}_0 \in B_0$, $\mathbf{x} = \text{IVP}_{\mathbf{f}}(\mathbf{x}_0, h)$ exists and $\mathbf{x}(h) \in B_1$. We provide a complete validated algorithm for this problem. Under the assumption (promise) that for all $\mathbf{x}_0 \in B_0$, $\text{IVP}_{\mathbf{f}}(\mathbf{x}_0, h)$ exists, we prove the halting of our algorithm. This is the first halting algorithm for IVP problems in such a general setting.

We also introduce novel techniques for subroutines such as StepA and StepB, and a scaffold datastructure to support our End Enclosure algorithm. Among the techniques are new ways refine full- and end-enclosures based on a **radical transform** combined with logarithm norms. Our preliminary implementation and experiments show considerable promise, and compare well with current validated algorithms.

1. Introduction

We consider the following system of first order ordinary differential equations (ODEs)

$$\mathbf{x}' = \mathbf{f}(\mathbf{x}) \tag{1}$$

where $\mathbf{x} = (x_1, \dots, x_n) \in C^1([0, h] \rightarrow \mathbb{R}^n)$ are functions of time and $\mathbf{x}' = (x'_1, \dots, x'_n)$ indicate differentiation with respect to time, and $\mathbf{f} = (f_1, \dots, f_n) : \mathbb{R}^n \rightarrow \mathbb{R}^n$. Since this is an autonomous ODE, we may assume the initial time $t = 0$. Up to time scaling, we often assume that the end time is $h = 1$. This assumption is just for simplicity but our results and implementation allow any value of $h > 0$.

Given $\mathbf{p}_0 \in \mathbb{R}^n$ and $h > 0$, the **initial value problem** (IVP) for (\mathbf{p}_0, h) is the mathematical problem of finding a **solution**, i.e., a continuous function $\mathbf{x} : [0, h] \rightarrow \mathbb{R}^n$ that satisfies (1), subject to $\mathbf{x}(0) = \mathbf{p}_0$. Let $\text{IVP}_{\mathbf{f}}(\mathbf{p}_0, h)$ denote the set of all such solutions. Since \mathbf{f} is usually fixed or understood, we normally omit \mathbf{f} in our notations. We say that (\mathbf{p}_0, h) is **valid** if the solution exists and is unique, i.e., $\text{IVP}(\mathbf{p}_0, h) = \{\mathbf{x}_0\}$ is a singleton. In this case, we write $\mathbf{x}_0 = \text{IVP}(\mathbf{p}_0, h)$. It is convenient to write $\mathbf{x}(t; \mathbf{p}_0)$ for $\mathbf{x}_0(t)$. See Figure 1 for the solution to the Volterra system (Eg 1 in Table 1). The IVP problem has numerous applications such as modeling physical, chemical and biological systems.

The mathematical IVP gives rise to a variety of algorithmic problems since we generally cannot represent a solution $\mathbf{x}_0 = \text{IVP}(\mathbf{p}_0, h)$ explicitly. We are interested in **validated algorithms** [24] meaning that all approximations must be explicitly bounded (e.g., numbers are enclosed in intervals). In this setting, we introduce the simplest *algorithmic* IVP problem, that of computing an enclosure for $\mathbf{x}(h; \mathbf{p}_0)$. In real world applications, only approximate values of \mathbf{p}_0 are truly meaningful because of modeling uncertainties. So we replace \mathbf{p}_0 by a **region** $B_0 \subseteq \mathbb{R}^n$: B_0 is a non-empty set like a box or ball. Let $\text{IVP}(B_0, h) := \bigcup_{\mathbf{p}_0 \in B_0} \text{IVP}(\mathbf{p}_0, h)$. Call $B_1 \subseteq \mathbb{R}^n$ an **end-enclosure** for $\text{IVP}(B_0, h)$ if B_1 contains the set $\{\mathbf{x}(h) : \mathbf{x} \in \text{IVP}(B_0, h)\}$. So our formal algorithmic problem is the following **End Enclosure Problem**:

[★]This document contain the results of the research funded by NSF Grant #CCF-2212462.

*Corresponding author

✉ bz2517@nyu.edu (B. Zhang); yap@cs.nyu.edu (C. Yap)

ORCID(s): 0009-0002-2619-9807 (B. Zhang); 0000-0003-2952-3545 (C. Yap)

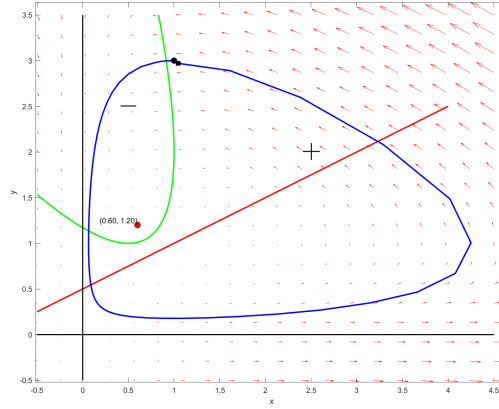


Figure 1: Volterra system (Eg1). The negative zone of the system is the region above the green parabola.

$\text{EndEnc}_f(B_0, \varepsilon_0) \rightarrow (\underline{B}_0, \overline{B}_1)$
INPUT: $\varepsilon_0 > 0$ and $B_0 \subseteq \mathbb{R}^n$ is a non-empty box
such that $\text{IVP}_f(B_0, 1)$ is valid.
OUTPUT: non-empty boxes $\underline{B}_0, \overline{B}_1$ in \mathbb{R}^n
with $\underline{B}_0 \subseteq B_0$, $w_{\max}(\overline{B}_1) < \varepsilon_0$, and
 \overline{B}_1 is an end-enclosure of $\text{IVP}_f(\underline{B}_0, 1)$.

(2)

This is basically the **Reachability Problem** in the non-linear control systems and verification literature (e.g., [34]). Our formulation of (2) has a natural but rare requirement that the end-enclosure \overline{B}_1 satisfies $w_{\max}(\overline{B}_1) < \varepsilon_0$. In order to achieve this, we must allow input B_0 to shrink to some \underline{B}_0 . But if we are promised that $\text{IVP}(B_0, 1)$ has an end-enclosure \overline{B}_1 with $w_{\max}(\overline{B}_1) < 2\varepsilon_0$, then it is possible to turn off shrinking and let $\underline{B}_0 = B_0$. In the common formulation of the IVP problem, B_0 is a singleton, $B_0 = \{p_0\}$. In this case, our algorithm will output $\underline{B}_0 = B_0$.

1.1. What is Achieved

Our formulation of the end-enclosure problem in (2) is new. We will present a complete validated algorithm for this problem. Our algorithm is **complete** in the sense that if the input is valid, then [C0] the algorithm halts, and [C1] if the algorithm halts, the output $(\underline{B}_0, \overline{B}_1)$ is correct. Algorithms that only satisfy [C1] are said¹ to be **partially correct**. To our knowledge, current validated IVP algorithms are only partially correct since halting is not proved.

The input to $\text{EndEnc1_IVP}_f(B_0, \varepsilon)$ assumes the validity of $(B_0, 1)$. All algorithms have requirements on their inputs, but they are typically syntax requirements which are easily checked. But validity of $(B_0, 1)$ is a semantic requirement which is non-trivial to check. Problems with semantic conditions on the input are called **promise problems** [12]. Many numerical algorithms are actually solutions of promise problems. Checking if the promise holds is a separate decision problem. To our knowledge, deciding validity of $(B_0, 1)$ is an open problem although some version of this question is undecidable in the analytic complexity framework [13, 19].

Hans Stetter [37] summarized the state-of-the-art over 30 years ago as follows: *To date, no programs that could be truly called 'scientific software' have been produced. AWA is state-of-the-art, and can be used by a sufficiently expert user – it requires selection of step-size, order and suitable choice of inclusion set representation.* Corliss [7, Section 10] made similar remarks. We believe our algorithm meets Stetter's and Corliss' criteria. The extraneous inputs such as step-size, order, etc, noted by Stetter are usually called **hyperparameters**. Our algorithm² does not require any

¹Completeness and partial correctness are standard terms in theoretical computer science.

²Hyperparameters are useful when used correctly. Thus, our implementation has some hyperparameters that may be used to improve performance, but they are optional and have no effect on completeness.

hyperparameters. Our preliminary implementation shows the viability of our algorithm, and its ability to do certain computations where current IVP software fails.

1.2. In the Shadow of Lohner’s AWA

In their comprehensive 1999 review, Nedialkov et al. [27] surveyed a family of validated IVP algorithms that may be³ called **A/B-algorithms** because each computation amounts to a sequence of steps of the form $\underbrace{ABAB \cdots AB}_{2m}$

$= (AB)^m$ for some $m \geq 1$, where A and B refer to two subroutines which⁴ we call `StepA` and `StepB`. It appears that all validated algorithms follow this motif, including Berz and Makino [21] who emphasized their `StepB` based on Taylor models. Ever since Moore [29] pointed out the **wrapping effect**, experts have regarded the mitigation of this effect as essential. The solution based on iterated QR transformation by Lohner [20] is regarded as the best technique to do this. It was implemented in the software called `AWA`⁵ and recently updated by Bungler [3] in a `INTLAB/MATLAB` implementation. The complexity and numerical issues of such iterated transformations have not been studied but appear formidable. See Revol [31] for an analysis of the special case of iterating a fixed linear transformation. In principle, Lohner’s transformation could be incorporated into our algorithm. By not doing this, we illustrate the extent to which other techniques could be used to produce viable validated algorithms.

In this paper, we introduce [N1] new methods to achieve variants of `StepA` and `StepB`, and [N2] data structures and subroutines to support more complex motifs than $(AB)^m$ above. Our algorithm is a synthesis of [N1]+[N2]. The methods under [N1] will refine full- and end-enclosures by exploiting `logNorm` and radical transforms (see next). Under [N2], we design subroutines and the scaffold data-structure to support new algorithmic motifs such as $(AB^+)^m$, i.e., A followed by one or more B ’s. Moreover, B^+ is periodically replaced by calling a special “`EulerTube`” to refine end-enclosures. This will be a key to our termination proof.

1.3. How to exploit Logarithmic Norm with Radical Transform

A **logNorm bound** of $B_1 \subseteq \mathbb{R}^n$ is any upper bound on

$$\mu_2(J_f(B_1)) := \sup \{ \mu_2(J_f(p)) : p \in B_1 \} \quad (3)$$

where J_f is the Jacobian of f and μ_2 is a `logNorm` function (Subsection 2.5). Unlike standard operator norms, `logNorm`s can be negative. We call B_1 a **contraction zone** if it has a negative `logNorm` bound. We exploit the fact that

$$\|x(t; p_0) - x(t; p_1)\| \leq \|p_0 - p_1\| e^{\bar{\mu}t}$$

(Theorem 4 in Subsection 2.5 where $\bar{\mu}$ is a `logNorm` bound). In the Volterra example in Figure 1, it can be shown that the exact contraction zone is the region above the green parabola. In tracing a solution $x(t; p_0)$ for $t \in [0, h]$ through a contraction zone, we can compute an end-enclosure B for IVP(B_0, h, B_1) with $w_{\max}(B) < w_{\max}(B_0)$ (i.e., the end-enclosure is “shrinking”). Previous authors have exploited `logNorm`s in the IVP problem (e.g., Zgliczynski [44], Neumaier [28]). We will exploit it in new way via a transform: for any box $B_1 \subseteq \mathbb{R}^n$, we introduce a “radical map” $\pi : \mathbb{R}^n \rightarrow \mathbb{R}^n$ (Section 5) with $y = \pi(x)$. Essentially, this transform is

$$y = (x_1^{-d_1}, \dots, x_n^{-d_n}) \quad (\text{for some } d_1, \dots, d_n \neq 0) \quad (4)$$

where $x = (x_1, \dots, x_n)$. The system $x' = f(x)$ transforms to another system $y' = g(y)$ in which the `logNorm` of $\pi(B_1)$ has certain properties (e.g., $\pi(B_1)$ is a contraction zone in the (y, g) -space). By computing end-enclosures in the (y, g) -space, we infer a corresponding end-enclosure in the (x, f) -space. Our analysis of the 1-dimensional case (Subsection 5.2), suggests that the best bounds are obtained when the `logNorm` of $\pi(B_1)$ is close to 0. In our current code, computing $\pi(B_1)$ is expensive, and so we avoid doing a transform if $\mu_2(J_f(B_1))$ is already negative.

1.4. Brief Literature Review

The validated IVP literature appeared almost from the start of interval analysis, pioneered by Moore, Eijgenraam, Rihm and others [10, 23, 24, 32]. Corliss [7] surveys this early period. Approaches based on Taylor expansion is

³This $(AB)^+$ motif is shared with homotopy path algorithms where A and B are usually called predictor and corrector (e.g., [41]).

⁴Nedialkov et al. called them Algorithms I and II.

⁵AWA abbreviates “Anfangswertaufgabe”, the German term for IVP.

dominant as they benefit from techniques such automatic differentiation and data structures such as the **Taylor model**. The latter, developed and popularized by Makino and Berz [3, 4, 21], has proven to be very effective. A major activity is the development of techniques to control the “wrapping effect”. Here Lohner’s approach [1, 20] has been most influential. Another advancement is the C^r -Lohner method developed by Zgliczyński et al. [44, 39]. This approach involves solving auxiliary IVP systems to estimate higher order terms in the Taylor expansion. The field of validated methods, including IVP, underwent great development in the decades of 1980-2000. Nedialkov et al provide an excellent survey of the various subroutines of validated IVP [17, 25, 26, 27].

In Nonlinear Control Theory (e.g., [11, 33]), the End-Enclosure Problem is studied under various **Reachability** problems. In complexity theory, Ker-i Ko [19] has shown that IVP is PSPACE-complete. This result makes the very strong assumption that the search space is the unit square ($n = 1$). Bournez et al [2] avoided this restriction by assuming that f has analytic extension to \mathbb{C}^d . In this paper, we adopt the “naive” but standard view of real computation throughout in order to avoid discussing arbitrary precision computation as in [19]; however all our methods only depend on interval bounds and full rigor can be achieved (cf. the AIE pathway in [42]).

The concept of **logarithmic norm**⁶ (or **logNorm** for short) was independently introduced by Germund Dahlquist and Sergei M. Lozinskiĭ in 1958 [35]. The key motivation was to improve bound errors in IVP. Neumaier [28] is one of the first to use logNorms in validated IVP. The earliest survey is T. Ström (1975) [38]. The survey of Gustaf Söderlind [35] extends the classical theory of logNorms to the general setting of functional analytic via Banach spaces.

One of the barriers to the validated IVP literature is cumbersome notations and lack of precise input/output criteria for algorithms. For instance, in the A/B algorithms, it is not stated if a target time $h > 0$ is given (if given, how it is used other than to terminate). Algorithm 5.3.1 in [27] is a form of StepA has a $\epsilon > 0$ argument but how it constrains the output is unclear; so it is unclear how to use this argument in the A/B algorithm. We provide a streamlined notation, largely by focusing on autonomous ODEs, and by introducing high-level data structures such as the scaffold. Besides non-halting and unclear input/output specification, another issue is the use of “failure modes” (e.g., [26, p.458, Figure 1]). Typical failure modes have no clear semantics but appear as an artifact of the implementation.

1.5. Paper Overview

The remainder of the paper is organized as follows: **Section 2** introduces some key concepts and computational tools. **Section 3** gives an overview of our algorithm. **Section 4** describes our StepA and StepB subroutines. **Section 5** describes our transform approach to obtain tighter enclosures. **Section 6** describes the Extend and Refine subroutines. **Section 7** presents our main algorithm and some global experiments. We conclude in **Section 8**. **Appendix A** gives all the proofs. **Appendix B** provide details of the affine transform $\bar{\pi}$.

2. Basic Tools

2.1. Notations and Key Concepts

We use bold fonts such as $\mathbf{x} = (x_1, \dots, x_n)$ or $\mathbf{p} \in \mathbb{R}^n$ for vectors. Vector–matrix or matrix–matrix products are indicated by \bullet (e.g., $A \bullet \mathbf{p}$ or $A \bullet B$). Let $\square \mathbb{R}^n$ denote the set of **boxes** in \mathbb{R}^n where each box B is a Cartesian product $B = \prod_{i=1}^n I_i$ and $I_i = [a_i, b_i]$, $a_i \leq b_i$. For any $S \subseteq \mathbb{R}^n$, let $Box(S)$ and $Ball(S)$ denote, respectively, the smallest box and the smallest Euclidean ball containing S . The Box and $Ball$ operators can take numerical parameters: if $\mathbf{r} = (r_1, \dots, r_n) \geq \mathbf{0}$ and $\mathbf{p} \in \mathbb{R}^n$, then

$$Box(\mathbf{r}) := \prod_{i=1}^n [-r_i, r_i], \quad Box_{\mathbf{p}}(\mathbf{r}) := \mathbf{p} + Box(\mathbf{r}).$$

We simply write $Box_{\mathbf{p}}(\mathbf{r})$ if $r_i = r$ for all i . For the box $B = Box_{\mathbf{p}}(\mathbf{r})$, its **midpoint** and **width** are $\mathbf{m}(B) := \mathbf{p}$ and $\mathbf{w}(B) := 2\mathbf{r}$, respectively. Similarly, $Ball_{\mathbf{p}}(r)$ is the ball centered at \mathbf{p} of radius r ; simply write “ $Ball(r)$ ” if \mathbf{p} is the origin $\mathbf{0}$. The **width** and **midpoint** of an interval $I = [a, b]$ is $w(I) := b - a$ and $m(I) := (a + b)/2$. The **width** and **midpoint** of a box $B = \prod_{i=1}^n I_i$ is $\mathbf{w}(B) := (w_1, \dots, w_n)$ and $\mathbf{m}(B) := (m_1, \dots, m_n)$, where $w_i = w(I_i)$ and $m_i = m(I_i)$. The **diameter** of B is $\|\mathbf{w}(B)\|_2 = \sqrt{\sum_{i=1}^n w_i^2}$. It follows that $Ball(B) = Ball_{\mathbf{m}(B)}(r(B))$, where $r(B)$ be half the diameter of B . Also define the **max-width** and **min-width** of B as $w_{\max}(B) := \max_{i=1}^n w(I_i)$, $w_{\min}(B) := \min_{i=1}^n w(I_i)$. We use the Euclidean norm on \mathbb{R}^n , writing $\|\mathbf{p}\| = \|\mathbf{p}\|_2$. If $S \subseteq \mathbb{R}^n$, then let $\|S\| := \sup \{\|\mathbf{p}\| : \mathbf{p} \in S\}$. For any function

⁶This concept goes by other names, including logarithmic derivative, matrix measure and Lozinskiĭ measure.

$f : X \rightarrow Y$, we re-use ‘ f ’ to denote its **natural set extension**, $f : 2^X \rightarrow 2^Y$ where 2^X is the power set of X and $f(S) = \{f(x) : x \in S\}$ for all $S \subseteq X$.

The **image** of a function $f : A \rightarrow B$ is $\text{image}(f) := \{f(a) : a \in A\}$. The **image** of $\text{IVP}(B_0, h)$ is the union $\bigcup_{x \in \text{IVP}(B_0, h)} \text{image}(x)$. A **full-enclosure** of $\text{IVP}(B_0, h)$ is a set $B_1 \subseteq \mathbb{R}^n$ that contains $\text{image}(\text{IVP}(B_0, h))$. We call (B_0, h, B_1) an **admissible triple** if (B_0, h) is valid and B_1 is a full-closure of $\text{IVP}(B_0, h)$. In this case, we can also write $\text{IVP}(B_0, h, B_1)$ for $\text{IVP}(B_0, h)$, and call (h, B_1) an **admissible pair** for B_0 . Finally, $\underline{B}_1 \subseteq B_1$ is an **end-enclosure** for $\text{IVP}(B_0, h, B_1)$ if for all solution $x \in \text{IVP}(B_0, h, B_1)$, we have $x(h) \in \underline{B}_1$. Call $(B_0, h, B_1, \underline{B}_1)$ an **admissible quadruple** (or quad).

2.2. Implicit use of Interval Computation

For any $g : \mathbb{R}^n \rightarrow \mathbb{R}$, a **box form** of g is any function $G : \square\mathbb{R}^n \rightarrow \square\mathbb{R}$ which is (1) conservative, and (2) convergent. This means (1) $g(B) \subseteq G(B)$ for all $B \in \square\mathbb{R}^n$, and (2) $g(p) = \lim_{i \rightarrow \infty} G(B_i)$ for any infinite sequence B_1, B_2, B_3, \dots that converges to a point $p \in \mathbb{R}^n$. In some proofs, it may appear that we need the additional condition, (3) that G is **isotone**. This means $B \subseteq B'$ implies $G(B) \subseteq G(B')$. In practice, isotony can often be avoided.

We normally denote a box form G of g by $\square g$ (if necessary, adding subscripts or superscripts to distinguish various box forms of g). See [15, 16]. In this paper, we will often ‘‘compute’’ exact bounds such as ‘‘ $f(E_0)$ ’’ (e.g., in StepA, Subsection 4.1). But in implementation, we really compute a box form $\square f(E_0)$. In the interest of clarity, we do not explicitly write $\square f$ since the mathematical function $f(E_0)$ is clearer.

2.3. Normalized Taylor Coefficients

For any solution x to the ODE (1), its i th **normalized Taylor coefficient** is recursively defined as follows:

$$f^{[i]}(x) = \begin{cases} x & \text{if } i = 0, \\ \frac{1}{i} \left(J_{f^{[i-1]}} \cdot f \right)(x) & \text{if } i \geq 1 \end{cases} \quad (5)$$

where J_g denotes the Jacobian of any function $g = g(x) \in C^1(\mathbb{R}^n \rightarrow \mathbb{R}^n)$ in the variable $x = (x_1, \dots, x_n)$. For instance, $f^{[1]} = f$ and $f^{[2]}(x) = \frac{1}{2}(J_f \cdot f)(x)$. It follows that the order $k \geq 1$ Taylor expansion of x at the point $t = t_0$ is

$$x(t_0 + h) = \left\{ \sum_{i=0}^{k-1} h^i f^{[i]}(x(t_0)) \right\} + h^k f^{[k]}(x(\xi)) \quad (6)$$

where $0 \leq \xi - t_0 \leq h$. If $x(\xi)$ lies in a box $B \in \square\mathbb{R}^n$, then interval form is

$$x(t_0 + h) \in \left\{ \sum_{i=0}^{k-1} h^i f^{[i]}(x(t_0)) \right\} + h^k f^{[k]}(B) \quad (7)$$

It is well-known that such Taylor coefficients can be automatically generated, and they can be evaluated at interval values using automatic differentiation.

2.4. Banach Space X_h

We give a brief summary of the basic theory. If X, Y are topological spaces, let $C^k(X \rightarrow Y)$ ($k \geq 0$) denote the set of C^k -continuous functions from X to Y . We fix $f \in C^k(\mathbb{R}^n \rightarrow \mathbb{R}^n)$ throughout the paper, and thus $k \geq 1$ is a global constant. It follows that $\text{IVP}_f(B_0, h) \subseteq C^k([0, h] \rightarrow \mathbb{R}^n)$. Let $X_h := C^k([0, h] \rightarrow \mathbb{R}^n)$. Then X_h is a real linear space where $c \in \mathbb{R}$ and $x, y \in X_h$ implies $cy \in X_h$ and $x \pm y \in X_h$. Let $\mathbf{0} \in X_h$ denote the additive identity in X_h : $x \pm \mathbf{0} = x$. Next X_h becomes a normed space with norm $\|x\|_{\max} := \max_{t \in [0, h]} \|x(t)\|_2$ where $\|\cdot\|_2$ is the 2-norm. If $S \subseteq X_h$, we let $\|S\|_{\max} := \sup_{x \in S} \|x\|_{\max}$. We turn X_h into a complete metric space (X_h, d) with metric $d(x, y) = \|x - y\|_{\max}$. Thus, X_h is a Banach space. To prove existence and uniqueness of solutions in X_h , we need a compact subset $Y_h \subseteq X_h$. Let $Y_h = Y_h(p_0, r) := \left\{ x \in C^1([0, h] \rightarrow \text{Ball}_{p_0}(r)) : x(0) = p_0 \right\}$. Then Y_h is also a complete metric space induced by X_h . The **Picard operator** on $T_f : X_h \rightarrow X_h$, is given by $T_f[x](t) = x(0) + \int_0^t f(x(s))ds$ for $x \in X_h$ and $t \in [0, h]$. We have 2 basic results:

(M) If $h < r/M$ where $M = \sup \left\{ \|f(p)\|_2 : p \in \text{Ball}_{p_0}(r) \right\}$, then $T_f[Y_h] \subseteq Y_h$, i.e., T_f is an endomorphism of Y_h .

(L) If we also have $h < L^{-1}$ where L is a Lipschitz constant for f on the ball $Ball_{p_0}(r)$, then T_f is a contraction map on Y_h , i.e., $\|T_f[\mathbf{x}] - T_f[\mathbf{y}]\|_{\max} < \|\mathbf{x} - \mathbf{y}\|_{\max}$.

It follows from (M) and (L) that there is unique $\mathbf{y}^* \in Y_h$ such that $T_f[\mathbf{y}^*] = \mathbf{y}^*$, i.e., \mathbf{y}^* is the unique fixed point of T_f . All this Banach space theory finally leads to the central result of IVP:

THEOREM 1 (Picard-Lindelöf Theorem). *Let $B = Ball_{p_0}(r) \subseteq \mathbb{R}^n$ be the ball centered at p_0 and $r > 0$. Then there exists $h > 0$ such IVP(p_0, h, B) is valid. In fact, it is sufficient to choose $h \leq \min\{r/M, 1/L\}$.*

For our algorithmic development, we need “constructive” tools to ensure the conditions of the Picard-Lindelöf theorem. The following is the key tool:

THEOREM 2 (Admissible Triple). *Let $f \in C^k(\mathbb{R}^n \rightarrow \mathbb{R}^n)$, $k \geq 1$ and $h > 0$. Let $F \subseteq \mathbb{R}^n$ be a compact convex set. If E_0 is contained in the interior of F_1 and satisfies the inclusion*

$$\sum_{i=0}^{k-1} [0, h]^i f^{[i]}(E_0) + [0, h]^k f^{[k]}(F_1) \subseteq F_1, \quad (8)$$

then (E_0, h, F_1) is an admissible triple.

Note that our result is very similar to the High-Order Enclosure Method (HOE) in [26, Theorem 4.1] who quoted [8, Theorem 3]. We give a self-contained proof in the appendix.

2.5. Logarithmic norms and Euler-tube Method

Let $\|A\|_p$ be the induced p -norm of a $n \times n$ matrix A with complex entries. Then the **logarithmic p -norm** of A is defined as

$$\mu_p(A) := \lim_{h \rightarrow 0^+} \frac{\|I + hA\|_p - 1}{h}.$$

We shall focus on $p = 2$, and call μ_2 the logNorm. E.g., if $n = 1$ then $A = a \in \mathbb{C}$ and $\mu_p(A) = \text{Re}(a)$. We have these bounds for logarithmic p -norms:

LEMMA 3.

- (a) $\mu_p(A + B) \leq \mu_p(A) + \mu_p(B)$
- (b) $\mu_p(A) \leq \|A\|_p$
- (c) $\mu_2(A) = \max_{j=1, \dots, k} (\frac{1}{2}(\lambda_j(A + A^T)))$ where $\lambda_1(A), \dots, \lambda_k(A)$ is the set of eigenvalues of A .
- (d) Let A be an $n \times n$ matrix and let $\max_{i=1}^n (\text{Re}(\lambda_i))$ where λ_i 's are the eigenvalues of A . Then
 - $\max_{i=1}^n (\text{Re}(\lambda_i)) \leq \mu(A)$ holds for any logNorm.
 - For any $\varepsilon \geq 0$, there exists an invertible matrix P such that

$$\max_i (\text{Re}(\lambda_i)) \leq \mu_{2,P}(A) \leq \max_i (\text{Re}(\lambda_i)) + \varepsilon.$$

where $\mu_{2,P}(A) := \mu_2(P^{-1}AP)$.

For parts(a-c) see [9], and part(d), see Pao [30]. In some estimates, we use these standard bounds:

$$\left. \begin{aligned} \|A\|_2 &= \max_i (\sqrt{\lambda_i(A^*A)}) \\ \|AB\|_2 &\leq \|A\|_2 \|B\|_2 \end{aligned} \right\} \quad (9)$$

We have the following result from Neumaier [28, Corollary 4.5, p. 331] (also [14, Theorem I.10.6]):

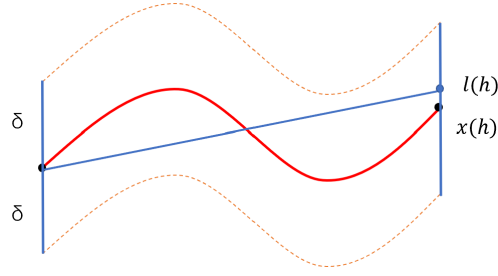


Figure 2: The dashed lines in the figure form a δ -tube around the red solid curve representing $\mathbf{x}(t)$. The segment $l(t)$ is a line segment inside this δ -tube.

THEOREM 4 (Neumaier).

Let $\mathbf{x} \in \text{IVP}_f(\mathbf{p}_0, h)$ and $\xi(t) \in C^1([0, h] \rightarrow \mathbb{R}^n)$ be any “approximate solution”.

Let⁷ P be an invertible matrix. Assume the constants $\varepsilon, \delta, \bar{\mu}$ satisfy

1. $\varepsilon \geq \|P^{-1} \cdot (\xi'(t) - f(\mathbf{x}(t)))\|_2$ for all $t \in [0, h]$
2. $\delta \geq \|P^{-1} \cdot (\xi(0) - \mathbf{x}(0))\|_2$
3. $\bar{\mu} \geq \mu_2(P^{-1} \cdot J_f(s\mathbf{x}(t) + (1-s)\xi(t)) \cdot P)$ for all $s \in [0, 1]$ and $t \in [0, h]$

Then for all $t \in [0, h]$,

$$\|P^{-1} \cdot (\xi(t) - \mathbf{x}(t))\|_2 \leq \begin{cases} \delta e^{\bar{\mu}t} + \frac{\varepsilon}{\bar{\mu}}(e^{\bar{\mu}t} - 1), & \bar{\mu} \neq 0, \\ \delta + \varepsilon t, & \bar{\mu} = 0. \end{cases} \quad (10)$$

COROLLARY 5. Let $\mathbf{x}_i \in \text{IVP}(\text{Ball}_{p_0}(r), h, F)$ for $i = 1, 2$ and $\bar{\mu} \geq \mu_2(J_f(F))$.

(a) For all $t \in [0, h]$,

$$\|\mathbf{x}_1(t) - \mathbf{x}_2(t)\|_2 \leq \|\mathbf{x}_1(0) - \mathbf{x}_2(0)\|_2 e^{\bar{\mu}t}. \quad (11)$$

(b) If $\mathbf{x}_1(0) = \mathbf{p}_0$ then an end-enclosure for $\text{IVP}(\text{Ball}_{p_0}(r), h, F)$ is

$$\text{Ball}_{\mathbf{x}_1(h)}(re^{\bar{\mu}h}).$$

Euler-tube Method: For any $\mathbf{x} \in \text{IVP}(E_0, h)$ and $\delta > 0$, the δ -tube of \mathbf{x} is the set

$$\text{Tube}_\delta(\mathbf{x}) := \{(t, \mathbf{p}) : \|\mathbf{p} - \mathbf{x}(t)\|_2 \leq \delta, 0 \leq t \leq h\} \quad (\subseteq [0, h] \times \mathbb{R}^n)$$

We say that a function $\ell : [0, h] \rightarrow \mathbb{R}^n$ belongs to the δ -tube of \mathbf{x} is for all $t \in [0, h]$, $(t, \ell(t)) \in \text{Tube}_\delta(\mathbf{x})$, see graph 2 for illustration.

LEMMA 6 (Euler Tube Method).

Let (B_0, H, B_1) be admissible triple, $\bar{\mu} \geq \mu_2(J_f(B_1))$ and $\bar{M} \geq \|f^{[2]}(B_1)\|$.

Consider the polygonal path $\mathbf{Q}_{h_1} = (\mathbf{q}_0, \mathbf{q}_1, \dots, \mathbf{q}_m)$ from the Euler method with m steps of uniform step-size h_1 given by

$$h_1 = h^{\text{euler}}(H, \bar{M}, \bar{\mu}, \delta) := \begin{cases} \min \left\{ H, \frac{2\bar{\mu}\delta}{\bar{M} \cdot (e^{\bar{\mu}H} - 1)} \right\} & \text{if } \bar{\mu} \geq 0 \\ \min \left\{ H, \frac{2\bar{\mu}\delta}{\bar{M} \cdot (e^{\bar{\mu}H} - 1) - \bar{\mu}^2\delta} \right\} & \text{if } \bar{\mu} < 0. \end{cases} \quad (12)$$

If each $\mathbf{q}_i \in B_1$ ($i = 0, \dots, m$) then the path \mathbf{Q}_{h_1} lies inside the δ -tube of $\mathbf{x}(t; \mathbf{q}_0)$. In other words, for all $t \in [0, H]$, we have

$$\|\mathbf{Q}_{h_1}(t) - \mathbf{x}(t; \mathbf{q}_0)\| \leq \delta. \quad (13)$$

⁷For our purposes, matrix P in this theorem can be the identity matrix.

This lemma gives us a technique to refine end- and full-enclosures (see Lemma 10 below).

3. Overview of our Algorithm

We will develop an algorithm for the End-Enclosure Problem (2), by elaborating on the classic Euler method or corrector-predictor framework for homotopy path (e.g., [36, 41]). The basic motif is to repeatedly call two subroutines⁸ which we call StepA and StepB, respectively:

$$\begin{array}{l}
\text{StepA}(E_0) \rightarrow (h, F_1): \\
\text{INPUT: } E_0 \in \square \mathbb{R}^n \\
\text{OUTPUT: an admissible pair } (h, F_1) \text{ for } E_0
\end{array} \tag{14}$$

$$\begin{array}{l}
\text{StepB}(E_0, h, F_1) \rightarrow (E_1): \\
\text{INPUT: } (E_0, h, F_1) \text{ is an admissible triple} \\
\text{OUTPUT: an end-enclosure } E_1 \text{ for IVP}(E_0, h)
\end{array} \tag{15}$$

Thus we see this progression

$$E_0 \xrightarrow{\text{StepA}} (E_0, h_0, F_1) \xrightarrow{\text{StepB}} (E_0, h_0, F_1, E_1) \tag{16}$$

where StepA and StepB successively transforms E_0 to an admissible triple and quad. By iterating (16) with E_1 we can get to the next quad (E_1, h_1, F_2, E_2) , and so on. *This is the basis of most validated IVP algorithms.* We encode this as:

$$\begin{array}{l}
\text{standard_IVP}(E_0) \rightarrow B_* \\
\text{INPUT: } E_0 \subseteq \mathbb{R}^n \text{ where IVP}(E_0, 1) \text{ is valid.} \\
\text{OUTPUT: an end-enclosure of IVP}(E_0, 1). \\
\hline
t_1 \leftarrow 0 \\
F_0 \leftarrow E_0 \\
\text{While } (t_1 < 1) \\
\quad (h, F_1) \leftarrow \text{StepA}(E_0) \\
\quad h \leftarrow \min(h, 1 - t_1) \\
\quad t_1 \leftarrow t_1 + h \\
\quad E_0 \leftarrow \text{StepB}(E_0, h, F_1) \\
\text{Return } E_0
\end{array} \tag{17}$$

Note that the iteration of (16) above is not guaranteed to halt (i.e., to reach $t = 1$). Towards ensuring halting, we will strengthen StepA with this concept: let $\varepsilon = (\varepsilon_1, \dots, \varepsilon_n) \geq 0$. Call (h, F_1) an ε -admissible pair for E_0 if (h, F_1) is an admissible pair for E_0 and

$$\varepsilon_i \geq \sup_{p \in F_1} |(f^{[k]}(p))_i|, \quad (i = 1, \dots, n) \tag{18}$$

where $(x)_i$ is the i th component of a vector x . As usual, (E_0, h, F_1) is a ε -admissible triple iff (h, F_1) is a ε -admissible pair for E_0 . When $\varepsilon_i = \varepsilon$ for all i , then we simply say ε -admissible pair/triple. See Theorem 2 for the context of this definition. We modify StepA to produce ε -admissible pairs:

⁸Nedialkov et al. [27] call them Algorithms I and II.

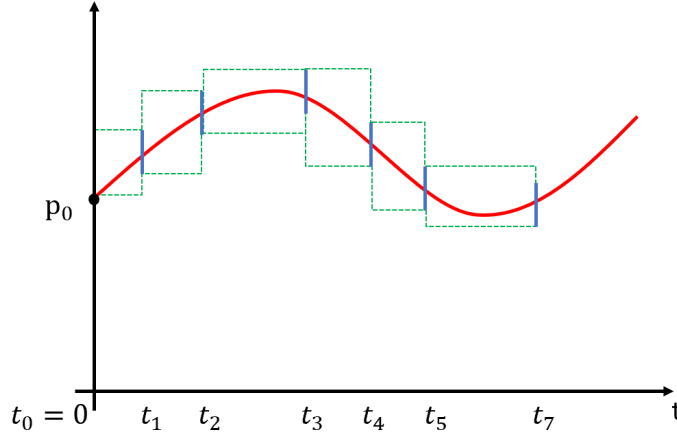


Figure 3: A 7-step scaffold. The horizontal axis represents time, and the vertical axis represents \mathbb{R}^n . The red curve corresponds to $x(t)$, the blue line segments represent end-enclosures, and the green boxes, represent full-enclosures.

StepA(E_0, ϵ, H) \rightarrow (h, F_1):
INPUT: $E_0 \in \square \mathbb{R}^n$, $0 < H \leq 1$ and $\epsilon \geq \mathbf{0}$
OUTPUT: an ϵ -admissible pair (h, F_1) for E_0
such that $h \leq H$.

(19)

3.1. Scaffold Data Structure

To go beyond the simple AB-iteration of (17), we introduce a data structure called a ‘‘scaffold’’ to encode the intermediate information needed for this computation. Figure 3 shows such a scaffold.

A **scaffold** with $m \geq 1$ **stages** is a quad $S = (t, \mathbf{E}, \mathbf{F}, \mathbf{G})$ where $t = (0 \leq t_0 < t_1 < \dots < t_m)$, $\mathbf{E} = (E_0, \dots, E_m)$, $\mathbf{F} = (F_1, \dots, F_m)$ and $\mathbf{G} = (G_1, \dots, G_m)$ such that for all $i = 1, \dots, m$,

$$(E_{i-1}, t_i - t_{i-1}, F_i, E_i) \text{ is an admissible quad} \quad (20)$$

and G_i is the i th **refinement substructure** whose discussion is deferred to Section 6. But basically, the time span $[t_{i-1}, t_i]$ will be refined into many mini-steps of uniform step sizes and G_i encodes this data. The quad in (20) is called the i th **quad** of S , also denoted

$$(E_{i-1}(S), \Delta t_i(S), F_i(S), E_i(S)).$$

The **end-** and **full-enclosure** of S is E_m and F_m (respectively). The **time sequence** and **time-span** of S refer to t and $[t_0, t_m]$, respectively.

Observation: For each $i = 0, \dots, m$, $E[i]$ is an end enclosure of IVP($E[0], t[i]$).

This observation is an immediate consequence of the admissibility of (20).

Let S and S' be scaffolds with m and m' stages respectively:

- Call S' an **extension** of S if S is a prefix of S' . If $m' = m + 1$, then S' is a **simple extension**.
- Call S' a **refinement** of S if they have the same time sequence $t(S) = t(S')$ (so $m = m'$) and for each $i = 1, \dots, m$, we have $E_i(S') \subseteq E_i(S)$, and $F_i(S') \subseteq F_i(S)$.

How to use a scaffold S : We call 2 subroutines on S , to *extend* and to *refine* it. The extension/refinement subroutines are analogous to StepA/StepB. We invoke the Extend subroutine as follows:

$$S.\text{Extend}(\dots).$$

Here we view S as an object in the sense of Object-Oriented Programming Languages (OOPL). The dot-invocation (“object.subroutine”) allows the subroutine to modify the object. Here is the header for the `Extend` subroutine:

$$S.\text{Extend}(\varepsilon_0, H)$$

INPUT: scaffold S with m stages, $\varepsilon_0 > 0$, $H > t_m(S)$.

OUTPUT: S is modified to S' which is a simple extension of S such that $t_{m+1}(S') \leq H$.

(21)

Basically, `Extend` could be implemented by calling `StepA` followed by `StepB` to produce a new admissible quad. In previous approaches (exemplified by (17)), one basically keep calling `Extend` until the end-time of S reaches the desired target H . But to ensure halting, we now insist that S be sufficiently “refined” before it can be extended again. Sufficient means that the end-enclosure of the last stage of S satisfies $w_{\max}(E_m(S)) \leq \varepsilon_0$ where ε_0 is input in (2)). Here then is the header of the `Refine` subroutine:

$$S.\text{Refine}(\varepsilon_0)$$

INPUT: m -stage scaffold S and $\varepsilon_0 > 0$.

OUTPUT: S' is a refinement of S such that $w_{\max}(E_m(S')) \leq \varepsilon_0$.

(22)

Within the `Refine` procedure, we will refine the i th time-span $[t_{i-1}, t_i]$ (for $i = 1, 2, \dots$) using “light-weight” techniques to improve the full- and end-enclosures. Specifically, the interval is uniformly subdivided into mini-step size h_i , and refinement is performed on such mini-intervals. Thus, we can refine the width of enclosures without modifying original time spans of the stages, allowing for more efficient and targeted refinement. See Section 6 below.

3.2. The Radical Transformation Method

We now introduce new techniques to compute enclosures more efficiently based on `logNorm` estimates via Theorem 4. Consider an admissible triple (E_0, h_1, F_1) . Let $\bar{\mu}$ be a logarithmic norm bound for (f, F_1) (see (3)). We briefly review the two methods.

The first method is based on the Euler-tube method: When the Euler step size is less than $h^{\text{euler}}(H, \bar{M}, \bar{\mu}, \delta)$ (see Lemma 6), we can invoke Corollary 5 to derive improved full- and end-enclosures for (E_0, h_1, F_1) . This solution lies inside an explicit δ -tube, a strong property we will need.

The second method is based on the **radical transformation** of the original system to reduce the logarithmic norm. We distinguish two cases:

Easy Case: $\bar{\mu} \leq 0$. In this case, F_1 is a contraction zone. By Theorem 4, we have $w_{\max}(E_1) \leq w_{\max}(E_0)$. Therefore, we directly estimate the full- and end-enclosures using the logarithmic norm without further transformation.

Hard Case: $\bar{\mu} > 0$. The key idea here is to construct an invertible transformation $\pi : \mathbb{R}^n \rightarrow \mathbb{R}^n$. Let $\mathbf{y} = (y_1, \dots, y_n) := \pi(\mathbf{x})$ and consider the transformed differential system:

$$\mathbf{y}' = \mathbf{g}(\mathbf{y}), \quad \mathbf{g}(\mathbf{y}) := J_{\pi}(\pi^{-1}(\mathbf{y})) \cdot \mathbf{f}(\pi^{-1}(\mathbf{y})). \quad (23)$$

This is considered with the admissible triple $(\pi(E_0), h, \pi(F_1))$.

We define the transformation as a composition:

$$\pi = \hat{\pi} \circ \bar{\pi}, \quad (24)$$

where $\bar{\pi}$ is an affine map (see Appendix B), and $\hat{\pi}(\mathbf{x}) = (x_1^{-d_1}, \dots, x_n^{-d_n})$ for some exponent vector $\mathbf{d} = (d_1, \dots, d_n)$ to be determined. The map $\hat{\pi}$ is invertible provided $d_i \neq 0$ for all i . Due to the component-wise inversion, we refer to π as the **radical transform**.

Assuming IVP (B_0, h, B_1) is valid (Section 2.1), and that B_1 is sufficiently small, we can show that $\pi(B_1)$ is a contraction zone for $(\pi(B_1), \mathbf{g})$. This brings the problem back to the easy case. After computing a shrunken enclosures in the transformed space, we pull it back to obtain an enclosures for the original IVP. For consistency, in the easy case, we define (π, \mathbf{g}) as (Id, \mathbf{f}) .

4. Steps A and B

Nedialkov et al [26, 27] provide a careful study of various algorithms for StepA and StepB. In the following, we provide new forms of StepA and StepB.

4.1. Step A

We now present an algorithm for StepA(E_0, H, ϵ). Its input/output specification has been given in (19). We can regard its main goal as computing the largest possible $h > 0$ (subject to $h \leq H$) such that (E_0, h, F_1) is ϵ -admissible for some F_1 . When calling StepA, we are at some time $t_1 \in [0, 1)$, and so the largest h we need is $H = 1 - t_1$. We therefore pass this value H to our subroutine. Our approach should be compared to [26, p.458, Figure 1], who uses a complicated heuristic formula for H based the previous step.

LEMMA 7.

Let $H > 0$, $\epsilon = (\epsilon_1, \dots, \epsilon_n)$, and $E_0 \subseteq \mathbb{R}^n$. Also let $\mathbf{M} = (M_1, \dots, M_n)$ with

$$M_i := \sup_{p \in \bar{B}} \left| (f^{[k]}(p))_i \right|, \quad (i = 1, \dots, n)$$

where $(\mathbf{x})_i$ is the i th coordinate of $\mathbf{x} \in \mathbb{R}^n$ and

$$\bar{B} := \sum_{i=0}^{k-1} [0, H]^i f^{[i]}(E_0) + \text{Box}(\epsilon).$$

If

$$h = \min \left\{ H, \min_{i=1}^n \left(\frac{\epsilon_i}{M_i} \right)^{1/k} \right\} \quad \text{and} \quad F_1 := \sum_{i=0}^{k-1} [0, h]^i f^{[i]}(E_0) + \text{Box}(\epsilon). \quad (25)$$

then (E_0, h, F_1) is an admissible triple.

Using Lemma 7, we can define StepA(E_0, H, ϵ) as computing (h, F_1) as given by (25). Call this the **non-adaptive** StepA, denoted StepA₀. This non-adaptive h may be too pessimistic. Instead, we will compute h adaptively:

```

StepA( $E_0, H, \epsilon$ )  $\rightarrow$  ( $h, F_1$ )
INPUT:  $E_0 \in \square \mathbb{R}^n$ ,  $H > 0$ ,  $\epsilon = (\epsilon_1, \dots, \epsilon_n)$ 
OUTPUT:  $0 < h \leq H$ ,  $F_1 \in \square \mathbb{R}^n$  such that  $(\text{int}(E_0), h, F_1)$  is  $\epsilon$ -admissible.

-----
 $h \leftarrow 0$ 
While ( $H > h$ )
   $F_1 \leftarrow \text{Box} \left( \sum_{i=0}^{k-1} [0, H]^i f^{[i]}(E_0) \right) + \text{Box}(\epsilon)$ 
   $\mathbf{M} \leftarrow \mathbf{w}(\text{Box}(f^{[k]}(F_1)))$ 
   $h \leftarrow \min \left\{ H, \min_{i=1}^n \left( \frac{\epsilon_i}{M_i} \right)^{1/k} \right\}$  (where  $\mathbf{M} = (M_1, \dots, M_n)$ )
   $\triangleleft$  Invariant:  $(E_0, h, F_1)$  is  $\epsilon$ -admissible
   $H \leftarrow H/2$ 
Return ( $h, F_1$ )

```

This is a bisection search for the “largest” h that satisfies the Lemma 7, i.e., such that (E_0, h, F_1) is ϵ -admissible. Within each iteration of the while-loop, the computed values of h and F_1 form an ϵ -admissible triple (E_0, h, F_1) (by Lemma 7). We halve H before repeating the while-loop – this ensures that the next value of h increases. We exit when $H \leq h$. Our experiments will show that our approach is highly effective.

LEMMA 8 (Correctness of StepA). StepA(E_0, H, ϵ) \rightarrow (h, F_1) is correct: i.e., the algorithm halts and outputs an ϵ -admissible triple (E_0, h, F_1) .

Implementation Notes: the code for StepA is written for readability, but easily modified to gain some efficiency:

- The summation $\sum_{i=0}^{k-1}$ in StepA should be evaluated with Horner's rule (see [26, p. 458]).
- We should pre-compute the values $D_i \leftarrow \mathbf{f}^{[i]}(E_0)$ (for $i = 0, \dots, k-1$) outside the while-loop. Inside the while-loop, we update F_1 using the formula $\text{Box}(\sum_{i=0}^{k-1} [0, H^i] D_i) + \text{Box}(\epsilon)$.

4.2. Step B

For Step B, there are several methods such as the ‘‘Direct Method’’ [25, 27], Lohner's method [20], and C^1 -Lohner method [40]. The Direct Method is basically the mean value form of Taylor expansion to order k . Given (E_0, h, F_1) , the Direct method given by Nedialkov [25, 27], returns

$$E_1 = \underbrace{\sum_{i=0}^{k-1} h^i \mathbf{f}^{[i]}(\mathbf{m}(E_0))}_{\text{Point}} + \underbrace{\left(\sum_{i=0}^{k-1} h^i J_{\mathbf{f}^{[i]}}(E_0) \right) \cdot (E_0 - \mathbf{m}(E_0))}_{\text{Centered Remainder}} + \underbrace{h^k \mathbf{f}^{[k]}(F_1)}_{\text{Full Remainder}} \quad (26)$$

$$= \underbrace{\sum_{i=0}^{k-1} h^i \mathbf{f}^{[i]}(\mathbf{m}(E_0)) + h^k \mathbf{f}^{[k]}(\mathbf{m}(F_1))}_{\text{Point}(q_0)} + \underbrace{\left(\sum_{i=0}^{k-1} h^i J_{\mathbf{f}^{[i]}}(E_0) \right) \cdot (E_0 - \mathbf{m}(E_0)) + h^k \mathbf{f}^{[k]}(F_1 - \mathbf{m}(F_1))}_{\text{Centered Remainder}} \quad (27)$$

where the final expression (27) is obtained from (26) by writing the (Full Remainder) $h^k \mathbf{f}^{[k]}(F_1)$ as the sum $h^k \mathbf{f}^{[k]}(\mathbf{m}(F_1)) + h^k \mathbf{f}^{[k]}(F_1 - \mathbf{m}(F_1))$ is the sum of a point q_0 and a ‘‘centered remainder set’’. Note that q_0 is basically the order k Taylor expansion of the midpoint $\mathbf{m}(E_0)$. Both the Lohner and the C^1 -Lohner methods are refinements of the Direct method. The Lohner method aims to reduce the wrapping effect in the Remainder Set. The C^1 -Lohner method goes further by considering the limit when $k \rightarrow \infty$: then $V := \left(\sum_{i=0}^{\infty} h^i J_{\mathbf{f}^{[i]}} \right)$ satisfies another ODE: $V' = J_f \cdot V$. By solving this ODE, the method effectively computes a tighter end-enclosure.

For reference, the Direct Method based on (27) will be called ‘‘StepB₀’’, i.e., $\text{StepB}_0(E_0, h, F_1) \rightarrow E_1$. What we will call ‘‘StepB’’ is a simple modification of StepB₀ to include a logarithmic norm estimate from Corollary 5:

StepB(E_0, h, F_1) $\rightarrow E_2$
INPUT: A admissible triple (E_0, h, F_1)
OUTPUT: E_1 is an end-enclosure for (E_0, h, F_1) .

$$q_0 \leftarrow \sum_{i=0}^{k-1} (h^i \mathbf{f}^{[i]}(\mathbf{m}(E_0))).$$

$$E_1 \leftarrow q_0 + h^k \mathbf{f}^{[k]}(F_1) + \left(\sum_{i=0}^{k-1} h^i J_{\mathbf{f}^{[i]}}(E_0) \right) \cdot (E_0 - \mathbf{m}(E_0)).$$

$$\bar{\mu} \leftarrow \mu_2(J_f(F_1))$$

$$r_0 \leftarrow \frac{1}{2} \|\mathbf{w}(E_0)\|_2 e^{\bar{\mu} h}$$

$$B \leftarrow \text{Box}_{q_0}(r_0) + \text{Box}(h^k \mathbf{f}^{[k]}(F_1))$$
Return $E_2 \leftarrow E_1 \cap B$

LEMMA 9 (Correctness of StepB). StepB(E_0, h, F_1) $\rightarrow E_2$ is correct, i.e., E_2 is an end-enclosure for (E_0, h, F_1)

4.3. Refinements of Full and End Enclosures using Euler

So far, the full- and end-enclosures using Steps A and B are based on Taylor's formula. We now show how to refine such enclosures using Euler steps.

LEMMA 10 (1-Step Euler Enclosures with logNorm).

Consider an admissible triple (E_0, H, F_1) where $E_0 := \text{Ball}_{p_0}(r_0)$.

Let $\bar{\mu} = \mu_2(J_f(F_1))$, $\bar{M} = \|\mathbf{f}^{[2]}(F_1)\|$, and $\delta > 0$.

If $q_0 = p_0 + h_1 \mathbf{f}(p_0)$ is obtained from p_0 by an Euler step of size h_1 where $h_1 \leq h^{\text{euler}}(H, \bar{M}, \bar{\mu}, \delta)$ (see (12)), then:

A Novel Approach to Initial Value Problems

Eg*	Name	$f(x)$	Parameters	Box B_0	Reference
Eg1	Volterra	$\begin{pmatrix} ax(1-y) \\ -by(1-x) \end{pmatrix}$	$\begin{pmatrix} a \\ b \end{pmatrix} = \begin{pmatrix} 2 \\ 1 \end{pmatrix}$	$Box_{(1,3)}(0.1)$	[22], [3, p.13]
Eg2	Van der Pol	$\begin{pmatrix} y \\ -c(1-x^2)y-x \end{pmatrix}$	$c = 1$	$Box_{(-3,3)}(0.1)$	[3, p.2]
Eg3	Asymptote	$\begin{pmatrix} x^2 \\ -y^2 + 7x \end{pmatrix}$	N/A	$Box_{(-1.5,8.5)}(0.01)$	N/A
Eg4	Lorenz	$\begin{pmatrix} \sigma(y-x) \\ x(\rho-z)-y \\ xy-\beta z \end{pmatrix}$	$\begin{pmatrix} \sigma \\ \rho \\ \beta \end{pmatrix} = \begin{pmatrix} 10 \\ 28 \\ 8/3 \end{pmatrix}$	$Box_{(15,15,36)}(0.001)$	[3, p.11]

Table 1
List of IVP Problems

(a) **(δ -Tube)**

The linear function $\ell(t) := (1 - t/h_1)p_0 + (t/h_1)q_0$ lies in the δ -tube of $x_0 = IVP(p_0, H)$.

(b) **(End-Enclosure)**

Then $Ball_{q_0}(r_0 e^{\bar{\mu}h_1} + \delta)$ is an end-enclosure for $IVP(E_0, h_1)$.

(c) **(Full-Enclosure)**

The convex hull $CHull(Ball_{p_0}(r'), Ball_{q_0}(r'))$ where $r' = \delta + \max(r_0 e^{\bar{\mu}h_1}, r_0)$ is a full-enclosure for $IVP(E_0, h_1)$.

The refinement strategy for a stage: To exploit Lemma 10, we refine the i th stage by subdividing the time interval $[t_{i-1}, t_i]$ into 2^{ℓ_i} uniform Euler steps, where $(t_i - t_{i-1})/2^{\ell_i}$ is the i th **mini-step size**. Recall that if this mini-step size is smaller than $h_1 = h^{\text{euler}}(H, \bar{M}, \bar{\mu}, \delta)$ (see (12)), then the Euler trajectory remains inside the δ -tube around the exact solution $x(t; q_0)$. Here the parameters $H, \bar{M}, \bar{\mu}$ are taken from the data of the i th stage. In this case, we can compute a δ -bound end-enclosure. We denote by $\delta = \delta(G_i)$ the **Euler-tube target** associated with the i th stage, where G_i is the corresponding refinement substructure. For the final stage of an m -stage scaffold, we set $\delta(G_m) = \varepsilon_0$, the input tolerance of Refine.

We call this the EulerTube Subroutine. Empirically, this procedure becomes inefficient when \bar{M} and $\bar{\mu}$ are large. We therefore introduce an alternative adaptive method, called Bisection, to reduce \bar{M} and $\bar{\mu}$.

- **Bisection Method:** we subdivide the interval $[0, H]$ into 2^ℓ mini-steps of size $h_\ell := H/2^\ell$ (for $\ell = 1, 2, \dots$). At each **level** ℓ , we can compute full- and end-enclosures $(F_i[j], E_i[j])$ of the j th mini-step ($j = 1, \dots, 2^\ell$) using the following formulas:

$$F_i[j] \leftarrow \sum_{p=0}^{k-1} [0, h_\ell]^p f^{[p]}(E_i[j-1]) + [0, h_\ell]^k f^{[k]}(F_1), \quad (28)$$

and

$$E_i[j] \leftarrow \text{StepB}(E_i[j-1], h_\ell, F_i[j], \mu_2(J_f(F_i[j]))) \quad (29)$$

- When ℓ is sufficiently large, i.e., $h_\ell \leq h_i$, then we can call the EulerTube subroutine above. Our experiments show, this subroutine is more accurate.

4.4. List of Problems and Local Experiments on Steps A and B

Table 1 is a list of problems used throughout this paper for our experiments. In this subsection, we give “local” (single-step) experiments on the effectiveness of our Steps A and B. Later in Section 7, we will do “global” experiments based on our overall algorithm. We measure each technique by ratios denoted by σ , such that $\sigma > 1$ shows the effectiveness of the technique. Note that the gains for local experiments may appear small (e.g., 1.0001). But in global m -step experiment, this translates to $(1.0001)^m$ which can be significant.

First, in Table 2, we compare our StepA with the non-adaptive StepA₀. This non-adaptive StepA₀ is basically the algorithm⁹ in [26, p.458, Figure 1].

⁹We replace their $h_{j,0}$ by H , and $2h_{j,0}^k f^{[k]}(\tilde{Y}_{j-1})$ by ε .

Eg	E_0	ε	H	σ	τ	ρ	
Eg1	[0.9, 1.1], [2.9, 3.1]	0.1	1.0	38.5	1.15	3.05	
			10	2.22×10^6	1.06	3.84	
		0.0001	1.0	56.8	1.02	5.26	
	10		2.17×10^6	1.27	3.62		
	Eg1	[2, 4], [3, 5]	0.1	1.0	3.89×10^4	1.03	2.41
				10	1.89×10^8	1.18	3.17
0.0001			1.0	4.97×10^3	1.01	1.52	
		10	2.65×10^8	1.45	1.72		
Eg2		[-3.1, -2.9], [2.9, 3.1]	0.1	1.0	5.12×10^3	14.6	8.49
				10	3.50×10^{12}	10.2	13.1
	0.0001		1.0	5.58×10^3	1.00	8.49	
		10	4.24×10^{12}	7.35	10.4		
	Eg2	[-4, -2], [3, 5]	0.1	1.0	3.69×10^5	1.08	5.21
				10	1.90×10^{14}	1.19	7.41
0.0001			1.0	4.56×10^5	1.0	2.58	
		10	2.60×10^{14}	1.49	3.16		
Eg3		[-1.51, -1.49], [8.49, 8.51]	0.1	1.0	2.41×10^4	1.83	65.2
				10	2.24×10^9	1.49	30.5
	0.0001		1.0	3.23×10^4	1.005	129	
		10	2.28×10^9	1.81	161		
	Eg3	[-3.5, -3.4], [8.4, 8.5]	0.1	1.0	4.30×10^4	1.36	21.1
				10	3.00×10^9	1.11	26.2
0.0001			1.0	4.36×10^4	1.20	31.2	
		10	3.05×10^9	1.20	38.7		
Eg4		[14.999, 15.001], [14.999, 15.001], [35.999, 36.001]	0.1	1.0	2.98×10^3	1.00	59.9
				10	1.81×10^8	1.04	80.5
	0.0001		1.0	3.83×10^3	1.01	2050.88	
		10	2.84×10^8	1.03	1356.44		
	Eg4	[12, 15], [13, 15], [34, 36]	0.1	1.0	1.63×10^4	1.04	4.05
				10	8.70×10^8	1.08	5.52
0.0001			1.0	1.95×10^4	1.05	2.05	
		10	1.09×10^9	1.07	2.51		

Table 2

Comparison of StepA with StepA₀. Each row of the table is an experiment with one of our examples (Eg1, Eq2, etc), with the indicated values of (E_0, H, ε) . The key column is labeled $\sigma = h/h_0$, giving the ratio of the adaptive step size over the non-adaptive size.

Let (h_0, F_0) and t_0 be the admissible pair and computing time for StepA₀ (E_0, H, ε) . Let $(h, F), t$ be the corresponding values for StepA (E_0, H, ε) . The performance of these 2 algorithms can be measured by three ratios:

$$\rho := \frac{w_{\max}(F)}{w_{\max}(F_0)}, \quad \sigma := \frac{h}{h_0}, \quad \tau := \frac{t}{t_0}.$$

The most important ratio is σ , which we want to be as large as possible and > 1 . A large σ will make ρ and τ to be > 1 , which is not good when viewed in isolation. But such increases in ρ and τ , in moderation, is a good overall tradeoff.

Table 2 shows that StepA can dramatically increase the step size h without incurring a significant increase in computation time. So the adaptive version is highly effective and meaningful.

In the StepB experiments in Table 3, we look at two ratios:

1. $\sigma_1 = \frac{w_{\max}(E_1)}{w_{\max}(E_2)}$ is the maximum width from the C^r -Lohner algorithm (E_1) divided by that of our StepB (E_2).
2. $\sigma_2 = \frac{w_{\max}(DB_1)}{w_{\max}(B_1)}$ is the maximum width (DB_1) from StepB₀ (i.e., the Direct method) divided by that of (B_1) from our StepB.

The effectiveness of our StepB is indicated by when these ratios are greater than 1. For each example, we provide an admissible triple and compute the logarithmic norm $\mu \geq \mu_2(J_f(F_1))$.

The data in the Table 3 show that intersecting either the C^r -Lohner method or the Direct method with the estimate from Corollary 5 leads to tighter enclosures, with the improvement being especially pronounced for the Direct method. This effect becomes more noticeable as the step size increases.

The Table 4 compares various examples under a given (E_0, H, F_1) , showing the values of $h_1 = h^{\text{euler}}(H, \overline{M}, \overline{\mu}, \delta)$ computed for different choices of δ (see (12)). It also reports the ratio of the maximum widths of the full enclosures obtained using Lemma 10 and (28), respectively.

The data in Table 4 demonstrate that our method described in Lemma 10 yields a better full enclosure than the one obtained from (28). It is worth emphasizing that updating the full enclosure is important, as it allows us to reduce the value of logNorm, which in turn enables further tightening of the end enclosure during subsequent refinement steps.

Eg*	E_0	F_1	h	μ	σ_1	σ_2
Eg1	Box(0.6,1.2)(0.01)	(0.58, 1.17) ± (0.03, 0.04)	0.10	-0.23	1.10	1.13
		(0.575, 1.135) ± (0.065, 0.075)	0.22	-0.03	1.16	1.41
		(0.57, 1.105) ± (0.16, 0.135)	0.34	0.28	1.11	2.88
	Box(0.6,1.2)(10 ⁻⁴)	(0.585, 1.175) ± (0.015, 0.025)	0.10	-0.27	1.10	1.10
		(0.57, 1.115) ± (0.08, 0.095)	0.33	0.09	1.15	5.10
		(0.57, 1.105) ± (0.14, 0.125)	0.37	0.26	1.11	16.09
Eg2	Box(-3,3)(0.1)	(-3.00, 2.96) ± (0.105, 0.14)	0.003	7.18	1.01	1.00
		(-2.92, 2.47) ± (0.22, 1.13)	0.05	10.67	1.00	1.02
		(-2.895, 2.265) ± (0.295, 2.005)	0.08	14.33	1.00	1.07
	Box(-3,3)(10 ⁻⁴)	(-2.985, 2.925) ± (0.015, 0.075)	0.006	6.03	1.01	1.03
		(-2.895, 2.35) ± (0.185, 1.37)	0.085	11.79	1.00	2.25
		(-2.895, 2.265) ± (0.295, 2.005)	0.09	12.66	1.00	2.57
Eg3	Box(-1.5,8.5)(0.001)	(-1.495, 8.475) ± (0.015, 0.035)	0.0005	-2.12	1.00	1.01
		(-1.49, 8.315) ± (0.02, 0.205)	0.004	-1.99	1.00	1.10
		(-1.445, 7.055) ± (0.065, 3.115)	0.04	0.37	1.00	2.07
	Box(-1.5,8.5)(10 ⁻⁴)	(-1.495, 8.475) ± (0.005, 0.025)	0.0005	-2.15	1.00	1.02
		(-1.495, 8.31) ± (0.005, 0.20)	0.004	-2.08	1.00	1.50
		(-1.445, 7.055) ± (0.055, 3.105)	0.04	0.34	1.00	8.61
Eg4	Box(15,15,36)(0.001)	(14.855, 13.475, 37.085) ± (0.145, 1.595, 1.815)	0.024	3.19	1.35	1.52
		(14.74, 12.885, 37.23) ± (0.28, 2.325, 2.27)	0.027	3.67	1.36	1.80
		(14.665, 12.58, 37.275) ± (0.375, 2.74, 3.215)	0.031	3.98	1.37	2.58
	Box(15,15,36)(10 ⁻⁴)	(14.855, 13.475, 37.085) ± (0.145, 1.595, 1.815)	0.020	3.19	1.33	1.79
		(14.80, 13.16, 37.23) ± (0.21, 1.97, 2.27)	0.024	3.42	1.35	3.18
		(14.665, 12.58, 37.275) ± (0.375, 2.74, 3.215)	0.031	3.98	1.37	13.52

Table 3

Comparison of StepB with the Direct method and the C^r -Lohner algorithm. The key column is $\sigma_2 = \frac{w_{\max}(DB_1)}{w_{\max}(B_1)}$, which reflects the ratio of the maximum width produced by the Direct method (DB_1) to that by StepB (B_1), serving as a direct measure of their relative tightness. We also report σ_1 which compares the maximum width from the C^r -Lohner algorithm with that of the combined method based on Corollary 5.

Eg*	(E_0, H, F_1)			δ	h_1	μ	σ
	E_0	H	F_1				
Eg1	(1.0, 3.0) ± (0.1, 0.1)	0.1	(0.745, 2.955) ± (0.455, 0.295)	0.1	0.08	1.31	1.73
				0.01	0.008	1.31	1.09
				0.001	0.0008	1.31	1.01
Eg2	(-3.0, 3.0) ± (0.1, 0.1)	0.05	(-2.92, 2.40) ± (0.28, 0.80)	0.1	0.019	9.57	1.62
				0.01	0.0019	9.57	1.10
				0.001	0.00019	9.57	1.01
Eg3	(-1.50, 8.50) ± (0.01, 0.01)	0.04	(-1.445, 6.635) ± (0.165, 1.975)	0.1	0.0059	-0.0026	2.48
				0.01	0.00059	-0.0026	1.75
				0.001	0.000059	-0.0026	1.14
Eg4	(15.000, 15.000, 36.000) ± (0.001, 0.001, 0.001)	0.027	(14.736, 12.800, 37.279) ± (0.365, 2.301, 2.442)	0.1	0.0026	3.455	1.84
				0.01	0.00026	3.455	1.74
				0.001	0.000026	3.455	1.41

Table 4

Comparison of Full-Enclosures from Lemma 10 and (28). $\sigma := \frac{w_{\max}(F_0)}{w_{\max}(F)}$ where F is the enclosure computed via Lemma 10, and F_0 is the one obtained using (28).

5. Tighter Enclosures via Radical Transformation

In the previous section, we used the logNorm in combination with the Taylor method to obtain tighter enclosures. However, the earlier approach has two main issues:

1. It may only reduce the maximum width of the enclosure, without considering the minimum width.
For example, consider the ODE system $(x', y') = (7x, y)$, which consists of two independent one-dimensional subsystems. When analyzing this as a two-dimensional system, the logarithmic norm depends only on the component $x' = 7x$, since the logarithmic norm takes the maximum value.
2. For methods like the Direct method – which first track the midpoint and then estimate the range – there is a potential problem: the tracked midpoint can deviate significantly from the true center of the solution set. This deviation may lead to considerable overestimation in the resulting enclosure.

A radical map can be used to address these issues as suggested in our introduction.

Consider an admissible triple (E_0, h, F_1) . By the validity of IVP(E_0, h), the following condition can be achieved if E_0 sufficiently shrunk:

$$0 \notin \bar{F}_1 := \text{Box}(f(F_1)) = \prod_{i=1}^n \bar{I}_i. \tag{30}$$

This implies that there exists some $i = 1, \dots, n$ such that $0 \notin \bar{I}_i$. We need such a condition because the radical map (4) is only defined if each $x_i > 0$, which we can achieve by an affine transformation $\bar{\pi}$. Recall in Subsection 3.2 that in the hard case, we compute the map $\pi = \hat{\pi} \circ \bar{\pi}$ in (24). Define the box B_2 and \check{b}_{\max}

$$B_2 := \text{Box}(\bar{\pi}(F_1)) = \prod_{i=1}^n [1, \check{b}_i]. \quad \check{b}_{\max} := \max_{i=1, \dots, n} \check{b}_i. \quad (31)$$

Using $\bar{\pi}$, we can introduce a new ODE system

$$\bar{\mathbf{y}}' = \bar{\mathbf{g}}(\bar{\mathbf{y}}) \quad (32)$$

with new differential variables $\bar{\mathbf{y}} = (y_1, \dots, y_n)$ which are connected to (\mathbf{x}, \mathbf{f}) as follows:

$$\begin{aligned} \bar{\mathbf{y}} &:= \bar{\pi}(\mathbf{x}) && \text{(relation between } \bar{\mathbf{x}} \text{ and } \bar{\mathbf{y}}) \\ \bar{\mathbf{g}}(\bar{\mathbf{y}}) &:= J_{\bar{\pi}} \cdot \mathbf{f}(\bar{\pi}^{-1}(\bar{\mathbf{y}})) && (\bar{\mathbf{g}}(\bar{\mathbf{y}}) \text{ is new algebraic function constructed from } \bar{\pi} \text{ and } \mathbf{f}) \end{aligned}$$

and

$$\bar{\mathbf{g}}(\bar{\pi}(F_1)) \geq \mathbf{1} = [1, \dots, 1]. \quad (33)$$

Note that $(\pi(E_0), h, \pi(F_1))$ is an admissible triple in the (\mathbf{y}, \mathbf{g}) -space.

THEOREM 11 (Radical Transform).

(a) For any $\mathbf{d} = (d_1, \dots, d_n)$, we have

$$\begin{aligned} \mu_2(J_{\mathbf{g}}(\pi(F_1))) &\leq \max \left\{ \frac{-(d_i+1)}{\check{b}_i} : i = 1, \dots, n \right\} \\ &\quad + \max_{i=1}^n \{d_i\} \cdot \|J_{\bar{\mathbf{g}}}(\bar{\pi}(F_1))\|_2 \cdot \max_{i=1}^n \left\{ \frac{(\check{b}_i)^{d_i+1}}{d_i} \right\}. \end{aligned}$$

(b) If $d_1 = \dots = d_n = d$ then

$$\mu_2(J_{\mathbf{g}}(\pi(F_1))) \leq -(d+1) \frac{1}{\check{b}_{\max}} + (\check{b}_{\max})^{d+1} \|J_{\bar{\mathbf{g}}}(\bar{\pi}(F_1))\|_2.$$

Until now, the value of \mathbf{d} in the radical map $\hat{\pi}$ was arbitrary. We now specify $\mathbf{d} = \mathbf{d}(F_1)$. The definition of \mathbf{d} is motivated by Theorem 11. The optimal choice of \mathbf{d} is not obvious. So we make a simple choice by restricting $d_1 = \dots = d_n = d$. In this case, we could choose the upper bound of d :

$$\bar{d}(F_1) := \max \left\{ 1, \quad 2 \|J_{\bar{\mathbf{g}}}(\bar{\pi}(F_1))\|_2 - 1 \right\}. \quad (34)$$

LEMMA 12. If $d \geq \bar{d}(F_1)$, we have:

$$(a) \quad \mu_2(J_{\mathbf{g}}(\pi(F_1))) \leq (-2 + (\check{b}_{\max})^{d+2}) \cdot \frac{\|J_{\bar{\mathbf{g}}}(\bar{\pi}(F_1))\|_2}{\check{b}_{\max}}.$$

$$(b) \quad \text{If } \log_2(\check{b}_{\max}) < \frac{1}{d+2} \text{ then } \mu_2(J_{\mathbf{g}}(\pi(F_1))) < 0.$$

To use this lemma, we first check if choosing d to be $\bar{d}(F_1)$ satisfies $\mu_2(J_{\mathbf{g}}(\pi(F_1))) < 0$. If so, we perform a binary search over $d \in [1, \bar{d}(F_1)]$ to find an integer d such that $\mu_2(J_{\mathbf{g}}(\pi(F_1)))$ is negative and as close to zero as possible. Otherwise, $\pi = \text{Id}$. As seen in Subsection 5.2, this is a good strategy.

Given an admissible triple (E_0, h, F_1) , we introduce a subroutine called $\text{Transform}(\mathbf{f}, F_1)$ to convert the differential equation $\mathbf{x}' = \mathbf{f}(\mathbf{x})$ to $\mathbf{y}' = \mathbf{g}(\mathbf{y})$ according to above map π . However, this transformation depends on the condition (30). So we first define the following predicate $\text{AvoidsZero}(\mathbf{f}, F_1)$:

AvoidsZero(f, F_1) \rightarrow true or false.
 INPUT: $F_1 \subseteq \square \mathbb{R}^n$.
 OUTPUT: true if and only if $\mathbf{0} \notin \text{Box}(f(F_1))$.

Now we may define the transformation subroutine:

Transform($f, F_1, \bar{\mu}_1$) \rightarrow ($\pi, g, \bar{\mu}$)
 INPUT: $F_1 \subseteq \square \mathbb{R}^n$ and $\bar{\mu}_1 \geq \mu_2(J_f(F_1))$.
 OUTPUT: (π, μ, g) where
 π and g satisfy (24) and (23).

 If (AvoidsZero(f, F_1)=false & $\bar{\mu}_1 \leq 0$)
 Return (Id, $f, \bar{\mu}_1$)
 Compute $\bar{\pi}$ to satisfy (33)
 Compute π and g according (24) and (23).
 $\bar{\mu} \leftarrow \mu_2(J_g(\pi(B)))$.
 Return ($\pi, g, \bar{\mu}$)

5.1. Transformation of Error Bounds

We say that $B \subseteq \mathbb{R}^n$ is a δ -**bounded end-enclosure** for an admissible triple (E_0, h, F) if

- (i) (E_0, h, F, B) is admissible, and
 - (ii) $rad(B_0) \leq rad(E_0)e^{\mu_2(J_f(F)) \cdot h} + \delta$
- (35)

where $rad(S)$ is the radius of the circumball of S . Moreover, the i th stage (E_{i-1}, h_i, F_i, E_i) of a scaffold S is δ -**bounded** if E_i is a δ -bounded end-enclosure for (E_{i-1}, h_i, F_i) .

Given $\delta_x > 0$, we want to compute a transformation $\delta_x \mapsto \delta_y$ such that if B is a δ_y -bounded end-enclosure for $(\pi(E_0), h, \pi(F_1))$ in the (y, g) -space, then $\pi^{-1}(B)$ is a δ_x -bounded end-enclosure of (E_0, h, F_1) in the (x, f) -space. The following lemma achieves this:

LEMMA 13.

Let $y = \pi(x)$ and

$$\begin{aligned} x &= IVP_f(x_0, h, F_1), \\ y &= IVP_g(\pi(x_0), h, \pi(F_1)). \end{aligned}$$

For any $\delta_x > 0$ and any point $p \in \mathbb{R}^n$ satisfying

$$\|\pi(p) - y(h)\|_2 \leq \delta_y := \frac{\delta_x}{\|J_{\pi^{-1}}(\pi(F_1))\|_2},$$
(36)

we have

$$\|p - x(h)\|_2 \leq \delta_x.$$

This bound transformation $\delta_x \mapsto \delta_y$ in this lemma is encoded in the subroutine (37):

TransformBound(δ, π, F_1) \rightarrow δ'
 INPUT: $\delta > 0, \pi, F_1$ as above.
 OUTPUT: $\delta' > 0$ satisfying the corollary.
 If (π is the identity map)
 Return δ .
 Else
 Return $\frac{\delta}{\|J_{\pi^{-1}}(\pi(F_1))\|_2}$.

(37)

$d \setminus e$	-2.5	-2.0	-1.5	-1.0	-0.5	0.5	1.0	1.5	2.0	2.5
-3.5	52.6123	1.0000	1.0000	1.0000	1.0000	1.0000	1	1.0000	1.0000	1.0000
-3.0	23.8482	22.1158	1.0000	1.0000	1.0000	1.0000	1	1.0000	1.0000	1.0000
-2.5	10.8027	10.2084	9.3113	1.0000	1.0000	1.0000	1	1.0000	1.0000	1.0000
-2.0	4.8901	4.7089	4.4287	3.9948	1.0000	1.0000	1	1.0000	1.0000	1.0000
-1.5	2.2121	2.1707	2.1051	1.9992	1.8276	1.0000	1	1.0000	1.0000	1.0000
-1.0	1.0000	1.0000	1.0000	1.0000	1.0000	1.0000	1	1.0000	1.0000	1.0000
-0.5	1.0000	1.0000	1.0000	1.0000	1.0000	1.5647	1	1.0308	1.0168	1.0000
0.5	1.0000	1.0000	1.0000	1.0000	1.0000	1.0000	1	1.0798	1.0464	1.0037
1.0	1.0000	1.0000	1.0000	1.0000	1.0000	1.0000	1	1.0611	1.0594	1.0075
1.5	1.0000	1.0000	1.0000	1.0000	1.0000	1.0000	1	1.0474	1.0492	1.0118

Table 5

This is a table of the ratios $W(e, d)$ using our transform subroutines. The red entries are maximal for each column, and correspond to the choice $d = e - 1$. Note that we exclude the column for $e = 0$ since the ODE $x' = x^e = 1$ is independent of x . We also excluded the row for $d = 0$ as the radical transform $y = x^d = 1$ makes y independent of x . The column for $e = 1$ is literally 1 (other values written "1.0000" are generally approximations).

5.2. Transformation of Enclosures

Let (E_0, h, F_1) be an admissible triple that has been transformed into $(\pi(E_0), h, \pi(F_1))$. Thus we have a primal (\mathbf{x}, \mathbf{f}) -space and a transformed (\mathbf{y}, \mathbf{g}) -space where $\mathbf{y} = \pi(\mathbf{x})$. Our goal is to show how enclosures in the \mathbf{y} -space translate into enclosures in the \mathbf{x} -space.

Let $\bar{\mu}^1$ be the logNorm bound for (\mathbf{f}, F_1) and $\bar{\mu}^2$ be the corresponding bound for $(\mathbf{g}, \pi(F_1))$. Given $\delta_x > 0$, if we trace $m = m(E_0)$ to get a point \mathbf{Q} such that $\|\mathbf{Q} - \mathbf{x}(h; m)\| \leq \delta_x$ then

$$E_1^{\text{std}} := \text{Box}_{\mathbf{Q}} \left(r_0 e^{\bar{\mu}^1 h} + \delta_x \right). \quad (38)$$

as an end-enclosure for IVP(E_0, h, F_1), r_0 radius of the circumball of E_0 . Using our π -transform we can first compute a point \mathbf{q} such that $\|\mathbf{q} - \mathbf{y}(h)\| \leq \delta_y$ and take its inverse, or we can take the inverse of the end-enclosure in (\mathbf{y}, \mathbf{g}) -space. These two methods give us two end-enclosures:

$$\begin{aligned} E_1^{\text{xform1}} &:= \text{Box}_{\pi^{-1}(\mathbf{q})} \left(r_0 e^{\bar{\mu}^1 h} + \delta_x \right), \\ E_1^{\text{xform2}} &:= \pi^{-1} \left(\text{Box}_{\mathbf{q}} \left((r'_0 + d_m) e^{\bar{\mu}^2 h} + \delta_y \right) \right), \\ E_1^{\text{xform}} &:= E_1^{\text{xform1}} \cap E_1^{\text{xform2}} \end{aligned} \quad (39)$$

where r'_0 is the radius of the circumball of $\pi(E_0)$ and $d_m \geq \|\pi(m(E_0)) - m(\pi(E_0))\|$. To motivate these transforms, the following will analyze the situation in the special case $n = 1$.

EXAMPLE 1 (BENEFITS OF TRANSFORM ($n = 1$)). Consider the ODE $x' = x^e$ ($e \neq 0$) for e real with corresponding valid IVP(B_0, h) where $B_0 = 0.2 \pm 0.04$ and $h = 1$. Apply the radical transform $y = x^{-d}$ for some real $d \neq 0$. Then we see that $y' = \frac{d}{dx} (x^{-d}) \cdot x' = -dy \frac{-e+1+d}{d}$. Let $W(e, d) := \frac{w_{\max}(E_1^{\text{std}})}{w_{\max}(E_1^{\text{xform}})}$ denote the ratio of the widths of the end-enclosure using (38) and (39). Table 5 shows that the maximum value of $W(e, d)$ for a fixed $e \neq 1$ is achieved when $d = e - 1$, i.e., $y' = -d$. ■

5.2.1. Local Experiments on Efficacy of Transformed Bounds

We will compare E_1^{std} and E_1^{xform} using two independent ratios:

$$\rho(E_1^{\text{std}}, E_1^{\text{xform}}) := \left(\frac{w_{\max}(E_1^{\text{std}})}{w_{\max}(E_1^{\text{xform}})}, \frac{w_{\min}(E_1^{\text{std}})}{w_{\min}(E_1^{\text{xform}})} \right). \quad (40)$$

Our current experiments shows that the first ratio in $\rho(E_1^{\text{std}}, E_1^{\text{xform}})$ is always less than the second ratio, and for simplicity, we only show the second ratio, which is denoted by $\sigma(E_1^{\text{std}}, E_1^{\text{xform}})$ in the last column of Table 6.

Table 6 compares a single step of our transform method with the Standard method (38).

Eg*	E_0	F_1	h	$\bar{\mu}^1$	d	$\bar{\mu}^2$	$\sigma(E_1^{\text{std}}, E_1^{\text{xform}})$
Eg1-a	$Box_{(1,3)}(10^{-4})$	$(0.95, 2.95) \pm (0.05, 0.05)$	0.00001	0.07	17 1	-68.30 -5.82	1.0000 1.0006
Eg1-b	$Box_{(1,3)}(10^{-4})$	$(0.95, 2.95) \pm (0.05, 0.05)$	0.0028	0.07	17 1	-68.30 -5.82	1.0000 1.0000
Eg2-a	$Box_{(3,-3)}(10^{-4})$	$(2.95, -2.95) \pm (0.05, 0.05)$	0.00086	5.90	23 1	-140.80 -11.00	1.0002 1.0007
Eg2-b	$Box_{(3,-3)}(10^{-4})$	$(2.95, -2.85) \pm (0.05, 0.15)$	0.01	5.93	23 1	-370.14 -9.20	1.0321 1.0458
Eg3-a	$Box_{(3,-3)}(10^{-4})$	$(2.95, -2.95) \pm (0.05, 0.05)$	0.001	9.75	20 1	-177.05 -9.87	1.0000 1.0008
Eg3-b	$Box_{(3,-3)}(10^{-4})$	$(3.05, -2.80) \pm (0.15, 0.20)$	0.02	10.64	20 1	-163.12 -9.39	1.0035 1.0665
Eg4-a	$Box_{(1,0,3,0,1,0)}(10^{-4})$	$(0.95, 2.95, 0.95) \pm (0.05, 0.05, 0.05)$	0.001	13.60	58 1	-22.10 -2.97	1.0102 1.0186
Eg4-b	$Box_{(1,0,3,0,1,0)}(10^{-4})$	$(1.20, 3.30, 0.95) \pm (0.30, 0.40, 0.05)$	0.02	13.62	10 1	-6.01 -3.01	1.3286 1.3933

Table 6

Comparison of our transform method with E_1^{std} (38). The value δ is fixed at 10^{-7} throughout.

	E_0	0.00001	0.0001	0.001	0.01	0.1	0.2	0.4	0.6
Eg1	$Box_{(1,3)}(10^{-4})$	1.0006	1.0000	1.0000	1.0000	1.0000	1.0000	1.0000	1.0000
Eg2	$Box_{(3,-3)}(10^{-4})$	1.0001	1.0008	1.005	1.055	2.628	6.227	32.772	192.823
Eg3	$Box_{(3,-3)}(10^{-4})$	1.0005	1.0013	1.003	1.032	1.706	2.517	7.923	17.892
Eg4	$Box_{(1,3,1)}(10^{-4})$	1.0006	1.0015	1.016	1.156	1.737	3.022	9.027	27.283

Table 7

Comparison of our transform method with E_1^{std} (38). Under Increasing Step Sizes.

Each row represents a single experiment. The columns under (E_0, F_1, h) represent an admissible triple. The column under $\bar{\mu}^1$ (resp. $\bar{\mu}^2$) represents the logNorm bound of F_1 in the (\mathbf{x}, \mathbf{f}) -space (resp. $\pi(F_1)$ in the (\mathbf{y}, \mathbf{g}) -space). The d column refers to uniform exponent $\mathbf{d} = (d, \dots, d)$ of our radical transform. The last column $\sigma(E_1^{\text{std}}, E_1^{\text{xform}})$ is the most significant, showing the relative improvement of our method over E_1^{std} (38).

Table 7 further investigates the impact of the step size h on the improvement ratio. In this experiment, the initial box E_0 is fixed, while h is gradually increased (from 0.00001 to 0.6), and the corresponding changes in σ are observed.

From the experimental results, we can conclude the following:

1. Applying the transformation consistently yields a tighter end-enclosure. Moreover, this improvement appears to grow exponentially.
2. When the IVP system exhibits significantly faster growth in one coordinate direction over a certain step size range, the benefit of applying the transformation becomes increasingly pronounced as the step size grows. This is clearly observed in examples such as eg2, eg3, and eg4. The case of eg1 with a loop trajectory (see Figure 1), when the step size is small (e.g., $h = 0.00001$), the system is in the positive zone region, and the transformation has a slight noticeable effect. However, for larger step sizes, the trajectory enters the negative zone, where the transformation loses its effectiveness.

6. Extend and Refine Subroutines

In this section, we present algorithms for Extend and Refine as specified in equations (21)–(22). But we first need to describe the refinement substructure inside the scaffold; this was deferred from Subsection 3.1.

6.1. Refinement Substructure

Let $S = (\mathbf{E}, t, \mathbf{F}, \mathbf{G})$ be an m -stage scaffold as in (20)). So $t = (t_0 < t_1 < \dots < t_m)$ with the i -th quad is $(E_{i-1}, \Delta t_i, F_i, G_i)$. Here are the details¹⁰ of the i th refinement substructure G_i :

$$G_i = G_i(S) = ((\pi_i, \mathbf{g}_i), (\mathcal{E}_i, \bar{\mathbf{E}}_i, \bar{\mathbf{F}}_i), \bar{\mu}_i^1, \bar{\mu}_i^2, \delta_i, h_i^{\text{euler}}) \quad (41)$$

where:

[G0] The pair (π_i, \mathbf{g}_i) represents the radical transformation of the i th stage. More precisely, π_i is the map π in (24) that transforms the original ODE $\mathbf{x}' = \mathbf{f}(\mathbf{x})$ to $\mathbf{y}' = \mathbf{g}_i(\mathbf{y})$ where $\mathbf{y} = \pi_i(\mathbf{x})$ (see (23)).

¹⁰The first 2 components are computed only once; the remaining components (in red font) are updated with each phase of the refinement.

[G1] The triple $(\ell_i, \bar{E}_i, \bar{F}_i)$ is called the i th **mini-scaffold** where $\ell_i \geq 0$ called the **level**. The level starts from 0 and is incremented with each “phase” of Refine, and across multiple Refine’s. In other words, it is never reset.

[G2] The time span $[t_{i-1}, t_i]$ is subdivided into 2^{ℓ_i} minimesteps, each of minimestep size

$$\hat{h}_i := \Delta t_i / 2^{\ell_i}.$$

[G3] \bar{E}_i, \bar{F}_i are arrays of length 2^{ℓ_i} representing these 2^{ℓ_i} admissible quads

$$(\bar{E}_i[j-1], \hat{h}_i, \bar{F}_i[j], \bar{E}_i[j]), \quad (j = 1, \dots, 2^{\ell_i})$$

of stepsize \hat{h}_i , where $\bar{E}_i[0] = E_i(S)$ (cf. (20)). These arrays are updated in one of two ways: they are usually updated using Bisection, and periodically, by the Euler-tube Method.

[G4] $\bar{\mu}_i^1, \bar{\mu}_i^2$ are arrays of length 2^{ℓ_i} . For $j = 1, \dots, 2^{\ell_i}$, each $\bar{\mu}^1[j]$ is an upper bound on $\mu_2(J_f(\bar{F}_i[j]))$. Then $\bar{\mu}^2[j]$ is simply the transformed bound $\mu_2(J_g(\pi(\bar{F}_i[j])))$

[G5] Finally, the pair $(\delta_i, h_i^{\text{euler}})$ is used to trigger the periodic invocation of the Euler Tube method. These quantities are computed from (12) see Lemma 6 and are chosen so that, if the mini-step size \hat{h}_i does not exceed h_i^{euler} , the Euler Tube method constructs a δ_i -tube that contains the exact solution over the mini-step. In this case we invoke the Euler Tube method to update the enclosures using the δ_i -bounds. Immediately after the call we halve δ_i and recompute h_i^{euler} to determine the next trigger threshold. We perform these constructions in the transformed space of $y' = g(y)$, since we use (39) to get the tighter enclosures.

Remarks on Design: the strict separation of the scaffold stages (as represented by the fixed sequence $(t_0 < t_1 < \dots < t_m)$) from its minimesteps is motivated by the fact that the i th stage depends on the parameters (π_i, g_i) in [G0]. We need to compute π_i and g_i using symbolic methods¹¹ using symbolic manipulations of the expressions in f . Since this computation is expensive, we avoid splitting up stages into smaller stages. The trigger mechanism in [G5] allows us to combine the different powers of the Bisection and Euler Tube method (as each method is individually capable of reaching our termination goals). Bisection is unconditionally applicable to give enclosure bounds, but gives poorer bounds than Euler Tube. On the other hand, Euler Tube requires minimestep size to be less than h_i^{euler} , which may be pessimistically small.

6.2. Extend Subroutine

We now implement the $S.\text{Extend}()$ subroutine whose header (21) was described in the overview:

```

S.Extend( $\epsilon_0, H$ )
INPUT:  $m$ -stage scaffold  $S$ ,  $\epsilon > 0, H > 0$ .
OUTPUT:  $S'$  is a  $m+1$ -stage extension  $S$  such that
         $\Delta t_{m+1}(S') \leq H$ , and  $(\Delta t_{m+1}(S'), E_{m+1}(S'))$  is an  $\epsilon$ -admissible pair for  $E_m(S)$ .
-----
 $(\hat{h}, F_1) \leftarrow \text{StepA}(E_m(S), \epsilon_0, H)$ .
 $\bar{\mu}_1 \leftarrow \mu_2(J_f(F_1))$ .
 $E_1 \leftarrow \text{StepB}(E_m(S), \hat{h}, F_1)$ .
 $(\bar{\mu}_2, \pi, g) \leftarrow \text{Transform}(f, F_1, \bar{\mu}_1)$ .
 $\delta'_1 \leftarrow \text{TransformBound}(\epsilon_0, \pi, F_1)$ 
 $h_1 \leftarrow h^{\text{euler}}(\hat{h}, \|g^{[2]}(\pi(F_1))\|, \bar{\mu}_2, \delta'_1)$ .  $\leftarrow$  See (12).
Let  $S_{m+1} \leftarrow (t_m + h_1, E_1, F_1)$  and  $G_{m+1} \leftarrow ((\pi, g), (0, (E_m(S), E_1), (F_1)), \bar{\mu}_1, \bar{\mu}_2, \epsilon_0, h_1)$ .
Return  $S; (S_{m+1}, G_{m+1})$ .

```

It is a straightforward invocation of StepA to add a new stage to S , and StepB to compute an end-enclosure. NEEDS more explanation...

¹¹A numerical approach via automatic differentiation is, in principle possible, but it gives extremely poor bounds.

6.3. Refine Subroutine

Finally we implement the $S.\text{Refine}(\varepsilon_0)$ subroutine with the header (22) in the overview. It ensures that the end-enclosure of S has max-width $\leq \varepsilon_0$. Each iteration of the main loop of Refine is called a **phase**. If S has m stages, then in each phase, we process stages $i = 1, \dots, m$ in this order. Recall the¹² mini-scaffold $(\ell_i, \bar{E}_i, \bar{F}_i)$ of stage i above. This mini-scaffold has a uniform time step of size $(\Delta t_i) \cdot 2^{-\ell_i}$. See Figure 4 for illustration. We will call the following $S.\text{Bisect}(i)$ to perform a bisection of each mini-step:

```

S.Bisect(i)
  INPUT:  $i$  refers to the  $i$ th stage of  $S$ .
         Let  $((\pi_i, \mathbf{g}_i), (\ell_i, \bar{E}_i, \bar{F}_i), \bar{\mu}_i^1, \bar{\mu}_i^2, \delta_i, \hat{h}_i) \leftarrow G_i(S)$ 
         be the  $i$ th refinement substructure
  OUTPUT: each mini-step of the  $i$ th stage
         is halved and  $\bar{\mu}_i^1, E_i, F_i$  are updated.

-----
Initialize three new vectors  $\mu = [], E' = [E_i[0]]$  and  $F' = []$ .
 $h \leftarrow (\Delta t_i)2^{-\ell_i-1}$ 
For  $j = 1, \dots, 2^{\ell_i}$ ,
  ▷ First half of  $j$  step
   $tmpF_1 \leftarrow \sum_{i=0}^{k-1} ([0, h]^i f^{[i]}(E'.back()) + [0, h]^k f^{[k]}(F_i[j]))$ .
   $\mu' \leftarrow \mu_2(J_f(tmpF_1)); \mu.push\_back(\mu')$ .
   $E \leftarrow \text{StepB}(E'.back(), h, tmpF_1)$ .
   $E'.push\_back(E); F'.push\_back(tmpF_1)$ ;
  ▷ Second half of  $j$  step
   $tmpF_2 \leftarrow \sum_{i=0}^{k-1} ([0, h]^i f^{[i]}(E) + [0, h]^k f^{[k]}(F_i[j]))$ .
   $\mu' \leftarrow \mu_2(J_f(tmpF_2)); \mu.push\_back(\mu')$ .
   $E \leftarrow \text{StepB}(E, h, tmpF_2)$ 
   $E'.push\_back(E); F'.push\_back(tmpF_2)$ ;
 $(\bar{\mu}_i^1, \ell_i, \bar{E}_i, \bar{F}_i) \leftarrow (\mu, \ell_i + 1, E', F') \quad \triangleleft \text{mini-scaffold is updated}$ 

```

In the above code, we view μ, E' and F' as vectors in the sense of C++. We append an item E to the end of vector E' by calling $E'.push_back(E)$ and $E'.back()$ returns the last item. When $(\Delta t_i)2^{-\ell_i}$ is less than the bound in (12), instead of bisection, we can use the EulerTube subroutine (to be described next) to update the data $E_i(S), F_i(S), \bar{\mu}_i^1, \bar{\mu}_i^2$

```

S.EulerTube(i)
  INPUT:  $i$  refers to the  $i$ th stage of  $S$ .
  OUTPUT: refine the  $i$ th stage using Lemma 10,
         such that the  $i$ th stage is  $\delta(G_i(S))$ -bounded (see (35))
         (Note:  $E_i(S), F_i(S), G_i(S)$  are modified)

-----
Let  $(\pi, \mathbf{g}, \bar{\mu}^1, \bar{\mu}^2, \delta, \hat{h}, \ell, E, F)$  be  $G_i(S)$ 
Let  $Ball_p(r_0)$  be the circumscribing ball of  $E[0]$ 
and  $Ball_p(r'_0)$  be the circumscribing ball of  $\pi(E[0])$ .
 $\mathbf{q} \leftarrow \pi(\mathbf{p}), d \leftarrow \|\mathbf{q} - m(\text{Box}(\pi(E[0])))\|$ .
Let  $H$  be the step size each mini-step of  $S[i]$ .
For ( $j = 1, \dots, 2^\ell$ )
   $\mathbf{q} \leftarrow \mathbf{q} + \mathbf{g}(\mathbf{q})H$ ,
   $\delta_1 \leftarrow \text{TransformBound}(\delta, \pi, F[j])$ .
   $\bar{\mu}^2[j] \leftarrow \mu_2(J_g(\pi(F[j])))$ .
   $r_1 \leftarrow r_0 e^{j\bar{\mu}^1[j]H} + \delta; r'_1 \leftarrow (r'_0 + d)e^{j\bar{\mu}^2[j]H} + \delta_1$ 
   $B \leftarrow \text{Box}(r_1); B' \leftarrow \text{Box}(r'_1)$ .
   $F[j] \leftarrow F[j] \cap \pi^{-1}(\text{Box}(\text{center}(\pi(E[j-1]))) + B') + B, \mathbf{q} + B' \quad \triangleleft \text{Full-enclosure for mini-step}$ 
   $\bar{\mu}^1[j] \leftarrow \mu_2(J_f(F[j]))$ .
   $E[j] \leftarrow E[j] \cap \pi^{-1}(\mathbf{q} + B') \cap (\pi^{-1}(\mathbf{q}) + B). \quad \triangleleft \text{End-enclosure for mini-step}$ 

```

Observe that EulerTube performs all its Euler computation in transformed space, and only pulls back the enclosures back to primal space. It turns out that EulerTube is extremely efficient compared to Bisect, and moreover, it ensures that the i th stage is now δ_i -bounded.

We are ready to describe the Refine subroutine:

¹²Viewing the i th stage as a bigStep, the mini-scaffold represent smallSteps of the i th stage.

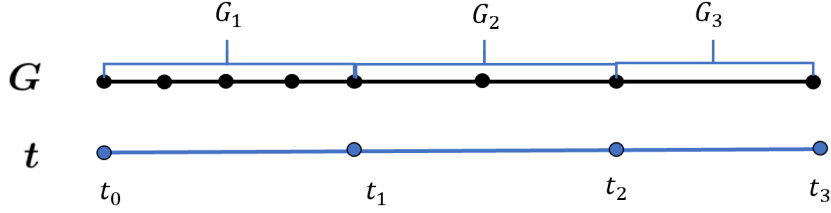


Figure 4: 3-stage scaffold S with $\ell_1 = 2$, $\ell_2 = 1$ and $\ell_3 = 0$ in G .

```

S.Refine( $\epsilon_0$ )
    INPUT:  $m$ -stage scaffold  $S$  and  $\epsilon_0 > 0$ .
    OUTPUT:  $S$  remains an  $m$ -stage scaffold
            that satisfies  $w_{\max}(E_m) \leq \epsilon_0$ .

     $r_0 \leftarrow w_{\max}(E_m(S))$ .
    While ( $r_0 > \epsilon_0$ )
        For ( $i = 1, \dots, m$ )  $\triangleleft$  Begin new phase
            Let  $\ell \leftarrow G_i(S).\ell$  and  $\Delta t_i \leftarrow t(S).t_i - t(S).t_{i-1}$ .
             $H \leftarrow (\Delta t_i)2^{-\ell}$ .
            If ( $H > \hat{h}$ )
                S.Bisect( $i$ )
            Else
                S.EulerTube( $i$ )
                Let  $G_i(S)$  be  $((\pi, g), (\ell, \bar{E}, \bar{F}), \bar{\mu}^1, \bar{\mu}^2, \delta, \hat{h})$  after the Euler Tube event.
                 $\triangleright$  We must update  $\delta$  and  $\hat{h}$  for the next Euler Tube event.
                 $G_i(S).\delta \leftarrow \delta/2$   $\triangleleft$  (Updating the  $\delta$  target is easy)
                 $\triangleright$  Updating  $\hat{h}$  to reflect the new  $\delta$  requires six preparatory steps: (1)–(6)
                (1)  $E_i(S) \leftarrow E[2^\ell]$   $\triangleleft$  End-enclosure for stage
                (2)  $F_i(S) \leftarrow \bigcup_{j=1}^{2^\ell} F[j]$   $\triangleleft$  Full-enclosure for stage
                (3)  $\mu_2^2 \leftarrow \max\{\bar{\mu}^2[j] : j = 1, \dots, 2^\ell\}$ 
                (4)  $\delta_1^i \leftarrow \text{TransformBound}(\delta, \pi, F_i(S))$  (cf. (37)).
                (5)  $\bar{M} \leftarrow \|g^{[2^i]}(\pi(F_i(S)))\|_2$ 
                (6)  $htmp \leftarrow \min\{\Delta t_i, h_{\text{euler}}(\hat{h}, \bar{M}, \mu_2^2, \delta_1^i)\}$   $\triangleleft$  (see Euler Tube lemma, Lemma 6)
                 $G_i(S).\hat{h} \leftarrow htmp$   $\triangleleft$  Finally, update  $\hat{h}$ 
             $\triangleleft$  End of For-Loop
             $E_0(S) \leftarrow \frac{1}{2}E_0(S)$ 
             $r_0 \leftarrow w_{\max}(E_m(S))$ 
         $\triangleleft$  End of While-Loop
    Return  $S$ 
    
```

THEOREM 14. *The subroutine $S.\text{Refine}(\epsilon_0)$ is correct. In particular, it halts.*

This proof is a bit subtle, and can be illustrated by the following **phase-stage** diagram:

	Stage 1	...	Stage i	...	Stage m
Phase 1:	δ_1^1	...	δ_i^1	...	ϵ_0
⋮	⋮	⋮	⋮	⋮	⋮
Phase k :	δ_1^k	...	δ_i^k	...	δ_m^k
⋮	⋮	⋮	⋮	⋮	⋮

(42)

Each phase will refine the stages $1, 2, \dots, m$ (in this order). The i th stage in phase k has a “target bound” $\delta_i^k > 0$ stored as $G_i(S).\delta$. For $k = 1$, δ_i^1 is ϵ_0 if $i = m$ and otherwise inherited from $(m - 1)$ -stage substructure before $\text{Extend}(\epsilon_0, H)$. For $k > 1$, δ_i^k halved after a call to EulerTube subroutine (see $\text{Refine}(\epsilon)$). The proof in the appendix will show that $\lim_{k \rightarrow \infty} \delta_i^k = 0$ for each $i = 1, \dots, m$, which will contradict the non-halting of Refine .

7. The Main Algorithm and Experiments

The following is our algorithm to solve the EndEnc1_IVP problem of (2):

```

EndEncf(B0, ε0) → (B̲0, B̄1):
INPUT: ε0 > 0, B0 ∈ □ℝn
      such that IVPf(B0, 1) is valid
OUTPUT: B̲0, B̄1 ∈ □ℝn, B̲0 ⊆ B0, wmax(B̄1) < ε
      and B̄1 is an end-enclosure of IVP(B̲0, 1)

```

```

S ← Init(f, B0, ε0)  ◀ Initialize a 0-stage scaffold
t ← 0
While t < 1
  S.Extend(ε0, 1 - t)
  S.Refine(ε0)
  t ← t(S).back()
Return (E0(S), E(S).back())

```

THEOREM 15. *Algorithm EndEnc(B₀, ε₀) halts, provided the interval computation of StepA is isotonic. The output is also correct.*

7.1. Implementation and Limitations

We implemented EndEnc in C++. Our implementation follows the explicitly described subroutines in this paper. There are no hidden hyperparameters (e.g., our step sizes are automatically adjusted). Our eventual code will be open-sourced in [6]. Implementation of the various numerical formulas such as Taylor forms implicitly call interval methods as explained in Subsection 2.2. The radical transform requires symbolic computation (Section 6) which we take from the symEngine library (<https://symengine.org/>).

Limitations. The main caveat is that we use machine arithmetic (IEEE standard). There are two main reasons. First, this is necessary to have fair comparisons to existing software and we rely on library routines based on machine arithmetic. In principle, we can implement our algorithm using arbitrary precision number types (which will automatically get a hit in performance regardless of needed precision).

7.2. Global Experiments

In previous sections, we had tables of experimental results evaluating “local” (1-step) operations. In this section, we show three tables (A, B, C) that solve complete IVP problems over time $t \in [0, 1]$ (with one exception in Table C). Table A compares our StepA/StepB with the standard methods. Table B is an internal evaluation of our transform and Bisect/EulerTube heuristic. Table C is an external comparison of our main algorithm with other validated software. The problems are from Table 1. We informally verify our outputs by tracing points using CAPD’s code to see that their outputs are within our end-enclosures. Timings are taken on a laptop with a 13th Gen Intel Core i7-13700HX 2.10 GHz processor and 16.0 GB RAM.

Our tables indicate two kinds of error conditions: **Timeout** and **No Output**. The former means the code took more than 1 hour to run. the latter means the code stopped with no output.

In each table, we are comparing our main enclosure algorithm denoted Ours with some algorithm X where X may be variants of Ours or other IVP software. We define **speedup over X** as $\sigma(X) := \frac{\text{Time}(X)}{\text{Time}(\text{Ours})}$.

TABLE A: We compare the relative computation times of Ours against Ours/StepA₀ and Ours/StepB₀. Here Ours/StepA₀ denotes the algorithm where we replace StepA by StepA₀ in Ours. Similarly for Ours/StepB₀. Recall StepA₀ is the non-adaptive stepA in Subsection 4.1, and StepB₀ is the direct method of (27). The speedup $\sigma(\text{Ours}/\text{StepB}_0)$ is a good measure of relative performance of StepB and StepB₀ when Ours and Ours/StepB₀ have about the same number of phases. So we include the statistic $\rho(\text{Ours}/\text{StepB}_0) := \frac{\text{phases}(\text{Ours}/\text{stepB}_0)}{\text{phases}(\text{Ours})}$.

We conclude from Table A that our StepA significantly improves efficiency ($\sigma(\text{Ours}/\text{StepA}_0)$). Moreover, StepB also yields a noticeable performance gain and effectively reduces the number of required phases ($\sigma(\text{Ours}/\text{StepB}_0)$ and $\rho(\text{Ours}/\text{StepB}_0)$).

TABLE B: We conduct experiments to show the benefits of various techniques used in our algorithm. The algorithms X being compared in Table B differ from Ours only in the use of variants of the Refine subroutine. Specifically: $X = \text{OurSimple}$ uses E_1^{std} (38) to compute the end-enclosure, without performing our Bisect

A Novel Approach to Initial Value Problems

Example	E_0	ϵ	Time(Durs)	$\sigma(\text{Ours}/\text{StepA}_0)$	$\sigma(\text{Ours}/\text{StepB}_0)$	$\rho(\text{Ours}/\text{StepB}_0)$
Eg1	$Box_{(1,3)}(0.1)$	0.1	0.018	5.44	1.00	4/4
		0.01	0.073	1.57	1.08	5/5
		0.001	0.643	2.465	1.75	8/7
		0.0001	12.803	1.49	1.03	9/9
Eg2	$Box_{(-3,3)}(0.1)$	0.1	0.031	653.22	1.00	4/4
		0.01	0.086	334.875	1.025	7/7
		0.001	1.437	> 1000	1.074	10/10
		0.0001	11.491	> 1000	1.102	13/13
Eg3	$Box_{(-1.5,8.5)}(0.01)$	10.0	0.043	> 1000	1.03	1/1
		5.0	0.027	> 1000	1.04	1/1
		1.0	0.022	> 1000	1.06	1/1
		0.1	2.159	> 1000	5.81	3/3
Eg4	$Box_{(15,15,36)}(0.001)$	10.0	0.142	> 1000	1.24	1/1
		5.0	0.130	> 1000	2.24	5/1
		1.0	0.122	> 1000	14.38	7/1
		0.1	0.205	> 1000	> 1000	Timeout

Table A: Comparison of StepA and StepB with StepA₀ and direct-method. all run with $order = 20$.

Eg	ϵ	B_0	Method	B_0	B_1	#(miniSteps)	Time(s)
$x' = x^2$	0.01	[0.8, 0.9]	OurSimple	0.8495 ± 0.0005	5.6665 ± 0.0045	20861	45.630
			OurSimpleT	0.8495 ± 0.0005	5.6665 ± 0.0045	18	11.854
			OurNoT	0.8495 ± 0.0005	5.6665 ± 0.0045	297	15.073
			OurNoEuler	0.8495 ± 0.0005	5.6665 ± 0.0045	31	71.846
			Ours	0.8495 ± 0.0005	5.6665 ± 0.0045	16	5.966
$x' = x^2$	0.001	[0.98, 0.99]	OurSimple	0.985 ± 0.0005	65.6665 ± 0.00035	128890	2104.03
			OurSimpleT	0.985 ± 0.0005	65.6665 ± 0.00035	103	31.898
			OurNoT	0.985 ± 0.0005	65.6665 ± 0.00035	22763	85.051
			OurNoEuler	0.985 ± 0.0005	65.6665 ± 0.00035	72489	327.89
			Ours	0.985 ± 0.0005	65.6665 ± 0.00035	105	49.861
Eg1	0.01	$Box_{(1,3)}(0.1)$	OurSimple	(0.995, 2.995) ± (0.005, 0.005)	(0.077, 1.4635) ± (0.001, 0.0035)	1454	13.877
			OurSimpleT	(0.995, 2.995) ± (0.005, 0.005)	(0.077, 1.4635) ± (0.001, 0.0035)	1888	15.370
			OurNoT	(0.995, 2.995) ± (0.005, 0.005)	(0.077, 1.4635) ± (0.001, 0.0035)	47	9.386
			OurNoEuler	(0.995, 2.995) ± (0.005, 0.005)	(0.077, 1.4635) ± (0.001, 0.0035)	47	9.415
			Ours	(0.995, 2.995) ± (0.005, 0.005)	(0.077, 1.4635) ± (0.001, 0.0035)	47	9.232
Eg2	0.1	$Box_{(-3,3)}(0.1)$	OurSimple	(-2.995, 3.0) ± (0.025, 0.025)	(-2.13, 0.56) ± (0.05, 0.02)	997	15.343
			OurSimpleT	(-2.995, 3.0) ± (0.025, 0.025)	(-2.13, 0.56) ± (0.05, 0.02)	1367	16.540
			OurNoT	(-2.995, 3.0) ± (0.025, 0.025)	(-2.13, 0.56) ± (0.05, 0.02)	14	14.785
			OurNoEuler	(-2.995, 3.0) ± (0.025, 0.025)	(-2.13, 0.56) ± (0.05, 0.02)	14	15.119
			Ours	(-2.995, 3.0) ± (0.025, 0.025)	(-2.13, 0.56) ± (0.05, 0.02)	14	14.590
Eg3	0.1	$Box_{(-1.5,8.5)}(0.01)$	OurSimple	(-1.495, 8.495) ± (0.005, 0.005)	(-0.595, -6.685) ± (0.005, 0.045)	2908	25.710
			OurSimpleT	(-1.495, 8.495) ± (0.005, 0.005)	(-0.595, -6.685) ± (0.005, 0.045)	3223	23.110
			OurNoT	(-1.495, 8.495) ± (0.005, 0.005)	(-0.595, -6.685) ± (0.005, 0.045)	35	23.773
			OurNoEuler	(-1.495, 8.495) ± (0.005, 0.005)	(-0.595, -6.685) ± (0.005, 0.045)	1034	455.548
			Ours	(-1.495, 8.495) ± (0.005, 0.005)	(-0.595, -6.685) ± (0.005, 0.045)	25	11.795
Eg4	5	$Box_{(15,15,36)}(0.001)$	OurSimple	(15, 15, 36) ± (0.0005, 0.0005, 0.0005)	(-6.94, 1.81, 35.52) ± (1.64, 2.33, 2.5)	26	294.019
			OurSimpleT	(15, 15, 36) ± (0.0005, 0.0005, 0.0005)	(-6.94, 1.81, 35.52) ± (1.64, 2.33, 2.5)	26	166.969
			OurNoT	(15, 15, 36) ± (0.0005, 0.0005, 0.0005)	(-6.945, 2.99, 35.14) ± (1.005, 2.15, 1.88)	61	146.360
			OurNoEuler	(15, 15, 36) ± (0.0005, 0.0005, 0.0005)	(-6.94, 1.81, 35.52) ± (1.64, 2.33, 2.5)	26	159.028
			Ours	(15, 15, 36) ± (0.0005, 0.0005, 0.0005)	(-6.945, 2.99, 35.14) ± (1.005, 2.15, 1.88)	61	123.64

Table B: The global effects of radical transform and bisection for our algorithm, all run with $order = 3$.

subroutine. $X = \text{OurSimpleT}$ is similar, except that we use E_1^{form} (39) instead. Similarly, $X = \text{OurNoT}$ represents a variant of our algorithm with the transform step disabled (i.e., the transformation π is set to the identity map). Finally, $X = \text{OurNoEuler}$ is our algorithm with EulerTube disabled.

We run all the experiments with order $k = 3$ because with high order (e.g. $k = 20$), the number of stages is too small (see Table C).

We conclude from Table B that the transform method improves efficiency overall (compare OurSimple vs. OurSimpleT, and Ours vs. OurNoT). In certain cases, such as the example $x' = x^2$ and Eg3, the transform method can significantly improve performance. For the two-dimensional examples, Eg1, Eg2 and Eg3, the comparison between OurSimpleT and Ours shows that our Bisect subroutine enhances the overall performance of the algorithm. Also, comparing OurNoEuler with Ours shows that EulerTube can significantly improve performance when there are many mini-steps (e.g., $x' = x^2$ and Eg3).

TABLE C: The time span is $t \in [0, 1]$ in all the experiments except for Eg1-b, where $t \in [0, 5.5]$ corresponding to one full loop. This is an example that AWA cannot solve [3, p. 13]. For each example of order $k = 20$, we use our algorithm to compute a scaffold $S(\epsilon_0)$ for an initial value of ϵ_0 ; subsequently, this scaffold is refined using a smaller ϵ_i ($i = 1, 2, \dots$) to obtain $S(\epsilon_1)$, $S(\epsilon_2)$, \dots . The total number of mini-steps in all the stages of $S(\epsilon_i)$ is shown in column #(miniSteps); the timing for each refinement is incremental time. This nice refinement feature gives us to better precision control with low additional cost after the initial S .

We compared our algorithm with 3 other algorithms:

The first algorithm CAPD is from [5] and github. In Table 7.2, we invoke the method ICn0deSo1ver with Taylor order 20, based on the C^r -Lohner algorithm [44, 18]. The method accepts an interval input such our B_0 .

Case	Method	ϵ	\underline{B}_0	\underline{B}_1	#(miniSteps)	Time(s)	$\sigma(X)$
Eg1-a	Ours	1.0	$Box_{(1.0,3.0)}(0.1)$	$(0.08, 1.46) \pm (0.06, 0.16)$	7	0.010	1
	Refine	0.05	$Box_{(1.0,3.0)}(0.05)$	$(0.08, 1.46) \pm (0.02, 0.05)$	13	0.009	N/A
	Refine	0.03	$Box_{(1.0,3.0)}(0.025)$	$(0.08, 1.46) \pm (0.006, 0.02)$	25	0.017	N/A
	StepB _{Direct}	N/A	N/A	$(0.08, 1.47) \pm (0.06, 0.15)$	N/A	0.014	1.4
	StepB _{Lohner}	N/A	N/A	$(0.08, 1.46) \pm (0.06, 0.15)$	N/A	0.031	3.1
Eg1-b	Ours	3.3	$Box_{(1.0,3.0)}(0.0125)$	$(0.95, 3.00) \pm (0.20, 0.30)$	294	0.404	1
	Refine	0.15	$Box_{(1.0,3.0)}(0.00625)$	$(0.95, 3.00) \pm (0.10, 0.14)$	587	0.326	N/A
	Refine	0.07	$Box_{(1.0,3.0)}(0.00313)$	$(0.95, 3.00) \pm (0.05, 0.7)$	1173	0.638	N/A
	StepB _{Direct}	N/A	N/A	Timeout	N/A	Timeout	-
	StepB _{Lohner}	N/A	N/A	Timeout	N/A	Timeout	-
Eg2	Ours	1.0	$Box_{(-3.1,3.1)}(0.1)$	$(-2.14, 0.57) \pm (0.28, 0.28)$	10	0.016	1
	Refine	0.1	$Box_{(-3.1,3.1)}(0.05)$	$(-2.14, 0.57) \pm (0.08, 0.04)$	19	0.012	N/A
	Refine	0.05	$Box_{(-3.1,3.1)}(0.025)$	$(-2.14, 0.57) \pm (0.03, 0.01)$	37	0.023	N/A
	StepB _{Direct}	N/A	N/A	$(-2.14, 0.57) \pm (0.26, 0.23)$	N/A	0.506	31.6
	StepB _{Lohner}	N/A	N/A	$(-2.14, 0.57) \pm (0.26, 0.23)$	N/A	0.904	56.5
Eg3	Ours	1.0	$Box_{(-1.51,8.51)}(0.01)$	$(-0.6, -6.69) \pm (0.00, 0.19)$	10	0.012	1
	Refine	0.06	$Box_{(-1.51,8.51)}(0.005)$	$(-0.6, -6.69) \pm (0.0008, 0.06)$	19	0.012	N/A
	Refine	0.03	$Box_{(-1.51,8.51)}(0.0025)$	$(-0.6, -6.69) \pm (0.0004, 0.02)$	37	0.022	N/A
	StepB _{Direct}	N/A	N/A	$(-0.60, -6.69) \pm (0.01, 0.19)$	N/A	4.113	342.7
	StepB _{Lohner}	N/A	N/A	$(-0.60, -6.69) \pm (0.01, 0.19)$	N/A	6.044	503.6
Eg4	Ours	4.5	$Box_{(15.0,15.0,36.0)}(0.001)$	$(-6.94, 2.99, 35.14) \pm (0.09, 0.15, 0.15)$	23	0.053	1
	Refine	0.6	$Box_{(15.0,15.0,36.0)}(0.0003)$	$(-6.94, 2.99, 35.14) \pm (0.05, 0.06, 0.06)$	89	0.161	N/A
	Refine	0.03	$Box_{(15.0,15.0,36.0)}(0.0001)$	$(-6.94, 2.99, 35.14) \pm (0.02, 0.02, 0.02)$	177	0.203	N/A
	StepB _{Direct}	N/A	N/A	$(-6.95, 3.00, 35.14) \pm (31.56, 176.50, 173.98)$	N/A	3.830	72.2
	StepB _{Lohner}	N/A	N/A	$(-6.95, 3.00, 35.14) \pm (31.23, 169.99, 166.39)$	N/A	8.398	158.4
	CAPD	N/A	N/A	$(-6.94, 2.99, 35.14) \pm (0.03, 0.01, 0.04)$	N/A	0.088	1.66

Table C: Experiments on EndEnc and Refine: comparison to CAPD and simple_IVP, all executed with $order = 20$.

$$\sigma(X) := \frac{\text{Time}(X)}{\text{Time}(\text{Ours})}.$$

The other two algorithms are simple_IVP algorithm in (17), where StepA is StepA₀ and StepB is either the StepB_{Direct} (see (27)) and well as StepB_{Lohner}. In Table 7.2, they are called StepB_{Direct} and StepB_{Lohner}, respectively.

We conclude from Table C that our method outperforms simple_IVP in terms of efficiency and is nearly as efficient as CAPD. Note that we deliberately choose ϵ so that our final \underline{B}_0 is equal to the input B_0 in order to be comparable to the other methods. The only case where $\underline{B}_0 \neq B_0$ is Eg1-b: here, our method successfully computes a solution while all the other methods fail to produce any output. Since our current method does not directly address the wrapping effect, the resulting end-enclosure is less tight than that of CAPD, as seen in Eg4. In addition, when higher precision (smaller ϵ) is required, our Refine algorithm can efficiently compute solutions to meet the desired accuracy.

8. Conclusion

We have presented a complete validated IVP algorithm with the unique ability to pre-specify the an ϵ -bound on the width of the end-enclosure. Preliminary implementations show promise in comparison to current validated software. This paper introduces a more structured approach to IVP algorithms, opening the way for considerable future development of such algorithms. We introduced several novel techniques for Step A and Step B, including a new exploitation of logNorms combined with the radical transform.

For future work, we plan to do a full scale implementation that includes the ability to use arbitrary precision arithmetic, in the style of Core Library [6, 43]. We will also explore incorporating the Lohner-type transform into our radical transform.:w

Nedialkov et al. [27, Section 10], “Some Directions for Future Research”, presented a list of challenges that remain relevant today. Our algorithm is one answer to their call for automatic step sizes, order control (interpreted as error control) and tools for quasi-monotone problems (i.e., contractive systems).

A. Appendix A: Proofs

The numberings of lemmas and theorems in this Appendix are the same as corresponding results in the text, and are hyperlinked to the text. Lemmas that do not appear the text are labeled as Lemma A.1, Lemma A.2, etc.

Theorem 2 (Admissible Triple)

Let $f \in C^k(\mathbb{R}^n \rightarrow \mathbb{R}^n)$, $k \geq 1$ and $h > 0$. Let $F \subseteq \mathbb{R}^n$ be a compact convex set. If E_0 is contained in the interior of F_1 and satisfies the inclusion

$$\sum_{i=0}^{k-1} [0, h]^i f^{[i]}(E_0) + [0, h]^k f^{[k]}(F_1) \subseteq F_1, \quad (43)$$

then (E_0, h, F_1) is an admissible triple.

Proof. Note that (8) implies that E_0 is contained in F_1 but not necessarily in the interior. Given $p_0 \in E_0$, there exists a solution $\mathbf{x} : [0, \tau) \rightarrow \mathbb{R}^n$ to the IVP given by $f' = f(\mathbf{x})$ and $\mathbf{x}(0) = p_0$. Assume that τ is maximal.

A1. If $\tau < \infty$ then $\mathbf{x}(\tau) = \infty$. By way of contradiction, assume $\mathbf{x}(\tau) \in \mathbb{R}^n$. By an application of Picard-Lindelöf's Theorem at $\mathbf{x}(\tau)$, we can extend the solution $\mathbf{x}(t)$ from $t = \tau$ to $t = \tau + \varepsilon$ for some $\varepsilon > 0$, contradicting the maximality of τ .

A2. For all $t \in [0, \min\{\tau, h\}]$, we have $\mathbf{x}(t) \in F_1$. Assume by way of contradiction that the set $S = \{t \in [0, \min\{\tau, h\}] : \mathbf{x}(t) \notin F_1\}$ is non-empty. Since S is bounded from below, $t^* = \inf S$ exists. Since $\mathbf{x}(0) \in E_0$ is in the interior of a convex set F_1 , this implies $t^* > 0$. For all $t \in [0, t^*)$, $\mathbf{x}(t)$ has the Taylor expansion

$$\left. \begin{aligned} \mathbf{x}(t) &= \left\{ \sum_{i=0}^{k-1} t^i f^{[i]}(p_0) \right\} + t^k f^{[k]}(\mathbf{x}(\xi)) && \text{(for some } \xi \in [0, t]; \text{ see (6))} \\ &\in \left\{ \sum_{i=0}^{k-1} h^i f^{[i]}(p_0) \right\} + [0, h]^k f^{[k]}(F_1) && (\mathbf{x}(\xi) \in F_1 \text{ since } \xi < t^* \leq h) \\ &\subseteq F_1 && \text{(by assumption (8)).} \end{aligned} \right\} \quad (44)$$

Thus $\mathbf{x}(t^*)$ is a limit point of $\{\mathbf{x}(t) : 0 \leq t < t^*\} \subseteq F_1$. By the compactness of F_1 , $\mathbf{x}(t^*) \in F_1$, contradicting A1.

A3. $h < \tau$. Otherwise, we have $\tau = \min\{\tau, h\}$ and A2 implies that for all $t \leq \tau$, $\mathbf{x}(t) \in F_1$. This means $\mathbf{x}(\tau) \in F_1$, contradicting A1.

A4. (E_0, h) is valid, i.e., for all $p_0 \in E_0$, $\text{IVP}(p_0, h)$ has a unique solution. From A3, we know that $\text{IVP}(p_0, h)$ is non-empty. Suppose $\mathbf{x}, \mathbf{y} \in \text{IVP}(p_0, h)$ with $\mathbf{x} \neq \mathbf{y}$. Let $t^\# := \inf\{t \in [0, h] : \mathbf{x}(t) \neq \mathbf{y}(t)\}$. Clearly $t^\#$ is well-defined. Moreover $\mathbf{x}(t^\#) = \mathbf{y}(t^\#)$ by continuity of solutions. Therefore the assumption $\mathbf{x} \neq \mathbf{y}$ implies $t^\# < h$. By Picard-Lindelöf (Theorem 1), there is a $h^\# > 0$ such $\text{IVP}(\mathbf{x}(t^\#), h^\#)$ has a unique solution \mathbf{z} . But this implies that $\mathbf{x}(t^\# + t) = \mathbf{y}(t^\# + t) = \mathbf{z}(t)$ for all $t \in [0, \min\{h^\#, h - t^\#\}]$. This contradicts the minimality $t^\#$.

A5. (E_0, h, F_1) is an admissible triple. We must show that for all $p_0 \in E_0$, F_1 is a full enclosure of $\text{IVP}(p_0, h)$. This follows from A2 and A3. **Q.E.D.**

Corollary 5

Let $\mathbf{x}_i \in \text{IVP}(\text{Ball}_{p_0}(r), h, F)$ for $i = 1, 2$ and $\bar{\mu} \geq \mu_2(J_f(F))$.

(a) For all $t \in [0, h]$,

$$\|\mathbf{x}_1(t) - \mathbf{x}_2(t)\|_2 \leq \|\mathbf{x}_1(0) - \mathbf{x}_2(0)\|_2 e^{\bar{\mu}t}. \quad (45)$$

(b) If $\mathbf{x}_1(0) = p_0$ then an end-enclosure for $\text{IVP}(\text{Ball}_{p_0}(r), h, F)$ is

$$\text{Ball}_{\mathbf{x}_1(h)}(re^{\bar{\mu}h}).$$

Proof. (a) Note that \mathbf{x}_1 and \mathbf{x}_2 are solutions of (1) with different initial values. We can apply Theorem 4 to bound $\|\mathbf{x}_1(t) - \mathbf{x}_2(t)\|$ by choosing $\delta = \|\mathbf{x}_1(0) - \mathbf{x}_2(0)\|$ and $\varepsilon = 0$. Then (10) implies

$$\begin{aligned} \|\mathbf{x}_1(t) - \mathbf{x}_2(t)\| &\leq \begin{cases} \delta e^{\bar{\mu}t} + \frac{\varepsilon}{\bar{\mu}}(e^{\bar{\mu}t} - 1) & \text{if } \bar{\mu} \neq 0, \\ \delta + \varepsilon t & \text{if } \bar{\mu} = 0 \end{cases} \\ &= \begin{cases} \delta e^{\bar{\mu}t} & \text{if } \bar{\mu} \neq 0, \\ \delta & \text{if } \bar{\mu} = 0 \end{cases} & (\text{since } \varepsilon = 0) \\ &= \|\mathbf{x}_1(0) - \mathbf{x}_2(0)\| e^{\bar{\mu}t} & (\text{for all } \bar{\mu}). \end{aligned}$$

By part (a), for any $\mathbf{q} \in \text{Ball}_{p_0}(r)$ the corresponding solution $\mathbf{y}(t) = \text{IVP}(\mathbf{q}, t)$ satisfies the perturbation estimate

$$\|\mathbf{x}_1(t) - \mathbf{y}(t)\| \leq r e^{\bar{\mu}t}, \quad \forall t \in [0, h].$$

Evaluating this inequality at $t = h$ gives

$$\|\mathbf{x}_1(h) - \mathbf{y}(h)\| \leq r e^{\bar{\mu}h}.$$

Thus $\mathbf{y}(h) \in \text{Ball}_{\mathbf{x}_1(h)}(r e^{\bar{\mu}h})$.

Q.E.D.

The following is a useful lemma:

Lemma A.2

Let (B_0, H, B_1) be an admissible triple with $\bar{\mu} \geq \mu_2(J_f(B_1))$, and $\bar{M} \geq \|f^{[2]}(B_1)\|$. Denote the Euler step at $\mathbf{q}_0 \in B_0$ by the linear function

$$\ell(t; \mathbf{q}_0) = \mathbf{q}_0 + t\mathbf{f}(\mathbf{q}_0).$$

Then for any $\mathbf{p}_0 \in B_0$ and $t \in [0, H]$,

$$\|\mathbf{x}(t; \mathbf{p}_0) - \ell(t; \mathbf{q}_0)\| \leq \|\mathbf{p}_0 - \mathbf{q}_0\| e^{\bar{\mu}t} + \frac{1}{2} \bar{M} t^2$$

Proof. By Corollary 5,

$$\|\mathbf{x}(t; \mathbf{p}_0) - \mathbf{x}(t; \mathbf{q}_0)\| \leq \|\mathbf{p}_0 - \mathbf{q}_0\| e^{\bar{\mu}t} \tag{46}$$

We also have

$$\begin{aligned} \mathbf{x}(t; \mathbf{q}_0) &= \mathbf{q}_0 + t \cdot \mathbf{f}(\mathbf{q}_0) + \frac{1}{2} t^2 \mathbf{x}''(\tau) \quad (\text{for some } \tau \in [0, t]) \\ \|\mathbf{x}(t; \mathbf{q}_0) - (\mathbf{q}_0 + t \cdot \mathbf{f}(\mathbf{q}_0))\| &\leq \left\| \frac{1}{2} t^2 \mathbf{x}''(\tau) \right\| \\ &= \left\| \frac{1}{2} t^2 \mathbf{f}^{[2]}(\mathbf{x}(\tau; \mathbf{q}_0)) \right\| \\ &\leq \left\| \frac{1}{2} t^2 \bar{M} \right\| & (\text{since } \bar{M} \geq \mathbf{f}^{[2]}(B_1)) \end{aligned}$$

Combined with (46), the triangular inequality shows our desired bound.

Q.E.D.

Lemma 6 Let (B_0, H, B_1) be an admissible triple, $\bar{\mu} \geq \mu_2(J_f(B_1))$ and $\bar{M} \geq \|f^{[2]}(B_1)\|$.

Consider the polygonal path $\mathcal{Q}_{h_1} = (\mathbf{q}_0, \mathbf{q}_1, \dots, \mathbf{q}_m)$ from the Euler method with m steps of uniform step-size h_1 given by

$$h_1 = h^{euler}(H, \bar{M}, \bar{\mu}, \delta) := \begin{cases} \min \left\{ H, \frac{2\bar{\mu}\delta}{\bar{M} \cdot (e^{\bar{\mu}H} - 1)} \right\} & \text{if } \bar{\mu} \geq 0 \\ \min \left\{ H, \frac{2\bar{\mu}\delta}{\bar{M} \cdot (e^{\bar{\mu}H} - 1) - \bar{\mu}^2 \delta} \right\} & \text{if } \bar{\mu} < 0. \end{cases} \tag{47}$$

If each $\mathbf{q}_i \in B_1$ ($i = 0, \dots, m$) then the path \mathbf{Q}_{h_1} lies inside the δ -tube of $\mathbf{x}(t; \mathbf{q}_0)$. In other words, for all $t \in [0, H]$, we have

$$\|\mathbf{Q}_{h_1}(t) - \mathbf{x}(t; \mathbf{q}_0)\| \leq \delta. \quad (48)$$

Proof. For simplicity, we only prove the lemma when H/h_1 is an integer. We first show that the Euler method with uniform step size h_1 has the following error bound:

$$\|\mathbf{q} - \mathbf{x}(H)\| \leq \begin{cases} \frac{\overline{M}h_1}{2\overline{\mu}}(e^{\overline{\mu}H} - 1) & \overline{\mu} \geq 0, \\ \frac{\overline{M}h_1}{2\overline{\mu} + \overline{\mu}^2 h_1}(e^{\overline{\mu}H} - 1) & \overline{\mu} < 0. \end{cases} \quad (49)$$

To show (49), assume the sequence $(\mathbf{q}_0 = \mathbf{x}(0), \mathbf{q}_1, \dots, \mathbf{q}_m = \mathbf{q})$ from the Euler method at times $t_0 = 0, t_1, \dots, t_m = H$. Let

$$g_i := \|\mathbf{q}_i - \mathbf{x}(t_i)\|_2, \quad i = 0, \dots, m.$$

By Lemma A.2 we obtain the linear recurrence

$$g_{i+1} \leq e^{\overline{\mu}h_1} g_i + \frac{\overline{M}h_1^2}{2}.$$

We solve this recurrence by induction. The base case $g_0 = 0$ holds by construction. Assume that for some $k \geq 0$ we have

$$g_k \leq \frac{\overline{M}h_1^2}{2} \sum_{j=0}^{k-1} e^{\overline{\mu}h_1 j}.$$

Then

$$\begin{aligned} g_{k+1} &\leq e^{\overline{\mu}h_1} g_k + \frac{\overline{M}h_1^2}{2} \\ &\leq e^{\overline{\mu}h_1} \cdot \frac{\overline{M}h_1^2}{2} \sum_{j=0}^{k-1} e^{\overline{\mu}h_1 j} + \frac{\overline{M}h_1^2}{2} \\ &= \frac{\overline{M}h_1^2}{2} \sum_{j=0}^k e^{\overline{\mu}h_1 j}. \end{aligned}$$

Hence, by induction we obtain

$$g_m \leq \frac{\overline{M}h_1^2}{2} \frac{e^{\overline{\mu}H} - 1}{e^{\overline{\mu}h_1} - 1}. \quad (50)$$

From (50) we deduce the following two useful bounds:

$$g_m \leq \begin{cases} \frac{\overline{M}h_1}{2\overline{\mu}}(e^{\overline{\mu}H} - 1), & \text{if } \overline{\mu} \geq 0, \\ \frac{\overline{M}h_1}{2\overline{\mu} + \overline{\mu}^2 h_1}(e^{\overline{\mu}H} - 1), & \text{if } \overline{\mu} < 0. \end{cases}$$

The first inequality follows from $e^{\bar{\mu}h_1} - 1 \geq \bar{\mu}h_1$ when $\bar{\mu} \geq 0$. For the second inequality (the case $\bar{\mu} < 0$) we use the elementary Taylor-type estimate $e^{\bar{\mu}h_1} - 1 \leq \bar{\mu}h_1 + \frac{1}{2}\bar{\mu}^2h_1^2$ (valid for $\bar{\mu}h_1 < 0$), which implies $e^{\bar{\mu}h_1} - 1 \leq \bar{\mu}h_1(1 + \frac{1}{2}\bar{\mu}h_1)$ and yields the stated bound.

Finally, by choosing h_1 as specified in (47), we ensure that $g_m < \delta$.

Q.E.D.

Lemma 7

Let $H > 0$, $\varepsilon = (\varepsilon_1, \dots, \varepsilon_n)$, and $E_0 \subseteq \mathbb{R}^n$. Also let $\mathbf{M} = (M_1, \dots, M_n)$ with

$$M_i := \sup_{p \in \bar{B}} \left| (f^{[k]}(p))_i \right|, \quad (i = 1, \dots, n)$$

where $(\mathbf{x})_i$ is the i th coordinate of $\mathbf{x} \in \mathbb{R}^n$ and

$$\bar{B} := \sum_{i=0}^{k-1} [0, H]^i f^{[i]}(E_0) + \text{Box}(\varepsilon).$$

If

$$h = \min \left\{ H, \min_{i=1}^n \left(\frac{\varepsilon_i}{M_i} \right)^{1/k} \right\} \quad \text{and} \quad F_1 := \sum_{i=0}^{k-1} [0, h]^i f^{[i]}(E_0) + \text{Box}(\varepsilon). \quad (51)$$

then (E_0, h, F_1) is an admissible triple.

Proof. Note that \bar{B} and F_1 are similar but one is based on H while the other is based on h . To prove the admissibility of (h, F_1) for E_0 , we invoke (8) and this fact:

$$[0, h]^k f^{[k]}(F_1) \subseteq \text{Box}(\varepsilon) = [\pm\varepsilon]. \quad (52)$$

Here is the proof of (52):

$$\begin{aligned} [0, h]^k f^{[k]}(F_1) &= [0, h]^k f^{[k]} \left(\sum_{i=0}^{k-1} [0, h]^i f^{[i]}(E_0) + [\pm\varepsilon] \right) && \text{(definition of } F_1) \\ &\subseteq [0, h]^k f^{[k]} \left(\sum_{i=0}^{k-1} [0, H]^i f^{[i]}(E_0) + [\pm\varepsilon] \right) && (h \leq H) \\ &= [0, h]^k f^{[k]}(\bar{B}) && \text{(definition of } \bar{B}) \\ &\subseteq [0, h]^k [-\mathbf{M}, \mathbf{M}] && \text{(definition of } \mathbf{M}) \\ &\subseteq [-\varepsilon, \varepsilon]. && \text{(definition of } h \text{ implies } h^k \mathbf{M} \leq \varepsilon) \end{aligned}$$

Q.E.D.

Lemma 8 (Correctness of StepA)

$\text{StepA}(E_0, H, \varepsilon) \rightarrow (h, F_1)$ is correct:

I.e., the algorithm halts and outputs an ε -admissible triple (E_0, h, F_1) .

Proof. The while-loop of StepA, we assert this invariant

$$(E_0, h, \bar{B}) \text{ is } \varepsilon\text{-admissible}$$

right after h is updated. This follows from Lemma 7. Let

$$(E_0, h_i, \bar{B}_i), \quad i = 1, 2, \dots$$

denote the admissible triple at the i th iteration. Thus, if the algorithm halts after the i th iteration, the output is admissible. It remains to show termination. Observe that

$$\overline{B}_1 \subset \overline{B}_2 \subset \dots$$

and therefore the h_i 's increases with i : $h_1 < h_2 < \dots$. Let $H_i = H/2^i$ be the value of H at the end of the i th iteration. Clearly, we enter the 1st iteration since H_0 is the input $H > 0$ and $h_0 = 0$. For $i \geq 1$, we enter the i th iteration iff $(H_{i-1} > h_{i-1})$ holds and we have:

$$0 = h_0 < h_1 < \dots < h_{i-1} < H_{i-1} < H_{i-2} < \dots < H_0$$

The while-loop must terminate since $H_i \rightarrow 0$ as $i \rightarrow \infty$ and $h_1 > 0$.

Q.E.D.

Lemma 9 (*Correctness of StepB*)

StepB(E_0, h, F_1) $\rightarrow E_2$ is correct, i.e., E_2 is an end-enclosure for (E_0, h, F_1)

Proof. The output E_2 is defined as the intersection $E_1 \cap B$. Since E_1 is already an end-enclosure for (E_0, h, F_1) by (27), it only remains to show that

$$B = \text{Box}_{q_0}\left(\frac{1}{2}\|w_{\max}(E_0)\| e^{\mu h}\right) + \text{Box}(h^k f^{[k]}(F_1))$$

is also an end-enclosure.

This follows directly from Corollary 5(b) together with the fact that the solution $\mathbf{x}_1 = \text{IVP}(m(E_0), h)$ satisfies

$$\mathbf{x}_1(h) \in q_0 + \text{Box}(h^k f^{[k]}(F_1)).$$

Q.E.D.

Lemma 10 Consider an admissible triple (E_0, H, F_1) where $E_0 := \text{Ball}_{p_0}(r_0)$.

Let $\bar{\mu} = \mu_2(J_f(F_1))$, $\overline{M} = \|f^{[2]}(F_1)\|$, and $\delta > 0$.

If $q_0 = p_0 + h_1 f(p_0)$ is obtained from p_0 by an Euler step of size h_1 where $h_1 \leq h^{\text{euler}}(H, \overline{M}, \bar{\mu}, \delta)$ (see (12)), then:

(a) (**δ -Tube**)

The linear function $\ell(t) := (1 - t/h_1)p_0 + (t/h_1)q_0$ lies in the δ -tube of $\mathbf{x}_0 = \text{IVP}(p_0, H)$.

(b) (**End-Enclosure**)

Then $\text{Ball}_{q_0}(r_0 e^{\bar{\mu} h_1} + \delta)$ is an end-enclosure for $\text{IVP}(E_0, h_1)$.

(c) (**Full-Enclosure**)

The convex hull $\text{CHull}(\text{Ball}_{p_0}(r'), \text{Ball}_{q_0}(r'))$ where $r' = \delta + \max(r_0 e^{\bar{\mu} h_1}, r_0)$ is a full-enclosure for $\text{IVP}(E_0, h_1)$.

Proof.

(a) By Lemma 6 we have $\ell(t)$ lies in the δ -tube of \mathbf{x}_0 , since for any $t \in [0, h_1]$, $\|\ell(t) - \mathbf{x}_0(t)\| \leq \delta$.

(b) By Corollary 5 we have for any $\mathbf{x} \in \text{IVP}(\text{Ball}_{p_0}(r_0), h_1, F_1)$, $\|\mathbf{x}(h_1) - \mathbf{x}_0(h_1)\| \leq r_0 e^{\bar{\mu} h_1}$. Since $\|q_0 - \mathbf{x}_0(h_1)\|_2 \leq \delta$, then by the triangular inequality we have

$$\|q_0 - \mathbf{x}(h_1)\|_2 \leq \|\mathbf{x}(h_1) - \mathbf{x}_0(h_1)\| + \|q_0 - \mathbf{x}_0(h_1)\|_2 \leq r_0 e^{\bar{\mu} h_1} + \delta,$$

so, $\mathbf{x}(h_1) \in \text{Ball}_{q_0}(r_0 e^{\bar{\mu} h_1} + \delta)$.

(c) We show that for any $T \in [0, h_1]$, the end-enclosure of $\text{IVP}(E_0, T)$ is a subset of $\text{Box}(\text{Ball}_{p_0}(r'), \text{Ball}_{q_0}(r'))$. Note that $E_1 = \text{Ball}_{\ell(T)}(r_0 e^{\bar{\mu}T} + \delta)$ is the end-enclosure for $\text{IVP}(E_0, T)$.

Let $\ell(T)_i$ denote the i -th component of $\ell(T)$ and $r(T) := r_0 e^{\bar{\mu}T} + \delta$. Then, we only need to prove that for any $i = 1, \dots, n$, the interval $\ell(T)_i \pm r(T)$ satisfies

$$\ell(T)_i \pm r(T) \subseteq \text{Box}((p_0)_i \pm (r' + \delta), (q_0)_i \pm (r' + \delta)),$$

where $(p_0)_i$ and $(q_0)_i$ are the i -th components of p_0 and q_0 , respectively.

Since $\ell(T)$ is a line segment, it follows that

$$\min((q_0)_i, (p_0)_i) \leq \ell(T)_i \leq \max((q_0)_i, (p_0)_i).$$

Additionally, we have $r(T) \leq r' + \delta$. Combining these observations, we conclude that

$$\ell(T)_i \pm r(T) \subseteq \text{Box}((p_0)_i \pm (r' + \delta), (q_0)_i \pm (r' + \delta)).$$

Q.E.D.

Lemma A.3

(a) $g(\mathbf{y}) = J_{\hat{\pi}}(\hat{\pi}^{-1}(\mathbf{y})) \cdot \bar{g}(\hat{\pi}^{-1}(\mathbf{y}))$

$$= \text{diag}(-d_i y_i^{1+\frac{1}{d_i}} : i = 1, \dots, n) \cdot \bar{g}(\hat{\pi}^{-1}(\mathbf{y})).$$

(b) The Jacobian matrix of g with respect to $\mathbf{y} = (y_1, \dots, y_n)$ is:

$$J_g(\mathbf{y}) = A(\mathbf{y}) + P^{-1}(\mathbf{y}) \cdot J_{\bar{g}}(\hat{\pi}^{-1}(\mathbf{y})) \cdot P(\mathbf{y}), \tag{53}$$

where

$$A(\mathbf{y}) = \text{diag}\left(- (d_i + 1) y_i^{\frac{1}{d_i}} \cdot (\bar{g}(\hat{\pi}^{-1}(\mathbf{y})))_i : i = 1, \dots, n\right)$$

and

$$P(\mathbf{y}) = \text{diag}\left(\frac{\bar{\pi}^{-1}(\mathbf{y})_i^{d_i+1}}{d_i} : i = 1, \dots, n\right).$$

Proof.

(a) For each $i = 1, \dots, n$, we have from (23) that $y'_i = g_i(\mathbf{y})$ where $\mathbf{y} = (y_1, \dots, y_n)$, $\mathbf{g} = (g_1, \dots, g_n)$, i.e.,

$$\begin{aligned} g_i(\mathbf{y}) = y'_i &= \left(\frac{1}{\bar{y}_i^{d_i}}\right)' \quad (\text{by (23) and } y_i = \bar{y}_i^{-d_i}) \\ &= -d_i \bar{y}_i^{-(d_i+1)} \bar{y}'_i \\ &= -d_i y_i^{1+\frac{1}{d_i}} \left(\bar{g}\left(y_1^{-\frac{1}{d_1}}, \dots, y_n^{-\frac{1}{d_n}}\right)\right)_i \\ &= -d_i y_i^{1+\frac{1}{d_i}} (\bar{g}(\hat{\pi}^{-1}(\mathbf{y})))_i. \end{aligned}$$

Thus,

$$g(\mathbf{y}) = (g_1(\mathbf{y}), \dots, g_n(\mathbf{y})) = \text{diag}(-d_i y_i^{1+\frac{1}{d_i}}, i = 1, \dots, n) \cdot \bar{g}(\hat{\pi}^{-1}(\mathbf{y}))$$

(b) By plugging $g_i(\mathbf{y}) = -d_i y_i^{1+\frac{1}{d_i}} (\bar{\mathbf{g}}(\bar{\pi}^{-1}(\mathbf{y})))_i$ into the Jacobian, we get

$$\begin{aligned} J_{\mathbf{g}}(\mathbf{y}) &= \begin{bmatrix} \nabla(g_1(\mathbf{y})) \\ \vdots \\ \nabla(g_n(\mathbf{y})) \end{bmatrix} = \begin{bmatrix} \nabla(-d_1 y_1^{1+\frac{1}{d_1}} (\bar{\mathbf{g}}(\bar{\pi}^{-1}(\mathbf{y})))_1) \\ \vdots \\ \nabla(-d_n y_n^{1+\frac{1}{d_n}} (\bar{\mathbf{g}}(\bar{\pi}^{-1}(\mathbf{y})))_n) \end{bmatrix} \\ &= \begin{bmatrix} \nabla(-d_1 y_1^{1+\frac{1}{d_1}} (\bar{\mathbf{g}}(\bar{\pi}^{-1}(\mathbf{y})))_1) \\ \vdots \\ \nabla(-d_n y_n^{1+\frac{1}{d_n}} (\bar{\mathbf{g}}(\bar{\pi}^{-1}(\mathbf{y})))_n) \end{bmatrix} + \begin{bmatrix} -d_1 y_1^{1+\frac{1}{d_1}} \nabla((\bar{\mathbf{g}}(\bar{\pi}^{-1}(\mathbf{y})))_1) \\ \vdots \\ -d_n y_n^{1+\frac{1}{d_n}} \nabla((\bar{\mathbf{g}}(\bar{\pi}^{-1}(\mathbf{y})))_n) \end{bmatrix} \end{aligned} \quad (54)$$

Note that for any $i = 1, \dots, n$,

$$\nabla(-d_i y_i^{1+\frac{1}{d_i}} (\bar{\mathbf{g}}(\bar{\pi}^{-1}(\mathbf{y})))_i) = (0, \dots, 0, -d_i \left(1 + \frac{1}{d_i}\right) y_i^{\frac{1}{d_i}} (\bar{\mathbf{g}}(\bar{\pi}^{-1}(\mathbf{y})))_i, \dots, 0)$$

and

$$\begin{aligned} -d_i y_i^{1+\frac{1}{d_i}} \nabla((\bar{\mathbf{g}}(\bar{\pi}^{-1}(\mathbf{y})))_i) &= \left(-d_i y_i^{1+\frac{1}{d_i}} \frac{\partial(\bar{\mathbf{g}}(\mathbf{x}))_i}{\partial x_j} (\bar{\pi}^{-1}(\mathbf{y})) \frac{\partial \bar{\pi}^{-1}(\mathbf{y})}{\partial y} : j = 1, \dots, n \right) \\ &= \left(\frac{d_i}{d_j} \begin{pmatrix} y_i^{1+\frac{1}{d_i}} \\ y_j \end{pmatrix} \frac{\partial(\bar{\mathbf{g}}(\mathbf{x}))_i}{\partial x_j} (\bar{\pi}^{-1}(\mathbf{y})) : j = 1, \dots, n \right) \\ &= \left(\frac{d_i}{d_j} \bar{\pi}^{-1}(\mathbf{y})_j^{d_j+1} \frac{\partial(\bar{\mathbf{g}}(\mathbf{x}))_i}{\partial x_j} (\bar{\pi}^{-1}(\mathbf{y})) \bar{\pi}^{-1}(\mathbf{y})_i^{-d_i-1} : j = 1, \dots, n \right). \end{aligned}$$

Thus,

$$J_{\mathbf{g}}(\mathbf{y}) = A(\mathbf{y}) + P^{-1}(\mathbf{y}) \cdot J_{\bar{\mathbf{g}}}(\bar{\pi}^{-1}(\mathbf{y})) \cdot P(\mathbf{y}),$$

where

$$A(\mathbf{y}) = \text{diag}(-(d_1 + 1) y_1^{\frac{1}{d_1}} (\bar{\mathbf{g}}(\bar{\pi}^{-1}(\mathbf{y})))_1, \dots, -(d_n + 1) y_n^{\frac{1}{d_n}} (\bar{\mathbf{g}}(\bar{\pi}^{-1}(\mathbf{y})))_n)$$

and

$$P(\mathbf{y}) = \text{diag}\left(\frac{\bar{\pi}^{-1}(\mathbf{y})_1^{d_1+1}}{d_1}, \dots, \frac{\bar{\pi}^{-1}(\mathbf{y})_n^{d_n+1}}{d_n}\right).$$

Q.E.D.

Theorem 11

(a) For any $\mathbf{d} = (d_1, \dots, d_n)$, we have

$$\begin{aligned} \mu_2(J_{\mathbf{g}}(\pi(F_1))) &\leq \max \left\{ \frac{-(d_i+1)}{\check{b}_i} : i = 1, \dots, n \right\} \\ &\quad + \max_{i=1}^n \{d_i\} \cdot \|J_{\bar{\mathbf{g}}}(\bar{\pi}(F_1))\|_2 \cdot \max_{i=1}^n \left\{ \frac{(\check{b}_i)^{d_i+1}}{d_i} \right\}. \end{aligned}$$

(b) If $d_1 = \dots = d_n = d$ then

$$\mu_2(J_{\mathbf{g}}(\pi(F_1))) \leq -(d + 1) \frac{1}{\check{b}_{\max}} + (\check{b}_{\max})^{d+1} \|J_{\bar{\mathbf{g}}}(\bar{\pi}(F_1))\|_2.$$

Proof. From **Lemma A.3(b)** we have for any $\mathbf{p} = (p_1, \dots, p_n) \in \bar{\pi}(F_1)$,

$$J_{\mathbf{g}}(\hat{\pi}(\mathbf{p})) = A(\mathbf{p}) + P^{-1}(\mathbf{p}) \frac{\partial \bar{\mathbf{g}}}{\partial \mathbf{x}}(\mathbf{p}) P(\mathbf{p}) \quad (55)$$

where $P(\mathbf{p}) = \text{diag}\left(\frac{p_i^{d_i+1}}{d_i} : i = 1, \dots, n\right)$ and $A(\mathbf{p}) = \text{diag}(a_1, \dots, a_n)$ with

$$a_i := -d_i\left(1 + \frac{1}{d_i}\right)p_i^{-1} \cdot (\bar{\mathbf{g}}(\mathbf{p}))_i. \quad (56)$$

Thus, A, P are diagonal matrices and P^{-1} is well-defined since $\mathbf{p} \in B_2 \geq \mathbf{1}$, (31).

By Lemma 3(b) and (56), we conclude that the form

$$\mu_2(A(\mathbf{p})) = \mu_2(\text{diag}(a_1, \dots, a_n)) = \max \{a_i : i = 1, \dots, n\}. \quad (57)$$

From (33), we conclude that

$$\begin{aligned} \mu_2(J_{\bar{\mathbf{g}}}(\widehat{\pi}(\mathbf{p}))) &= \mu_2\left(A(\mathbf{p}) + P^{-1}(\mathbf{p})\frac{\partial \bar{\mathbf{g}}}{\partial \mathbf{x}}(\mathbf{p})P(\mathbf{p})\right) \\ &\quad \text{(by (55))} \\ &\leq \mu_2(A(\mathbf{p})) + \mu_2\left(P^{-1}(\mathbf{p})\frac{\partial \bar{\mathbf{g}}}{\partial \mathbf{x}}(\mathbf{p})P(\mathbf{p})\right) \\ &\quad \text{(by Lemma 3(a))} \\ &\leq \mu_2(A(\mathbf{p})) + \left\|P^{-1}(\mathbf{p})\frac{\partial \bar{\mathbf{g}}}{\partial \mathbf{x}}(\mathbf{p})P(\mathbf{p})\right\|_2 \\ &\quad \text{(by Lemma 3(b))} \\ &\leq \max \left\{ \frac{-(d_i+1)}{b_i} : i = 1, \dots, n \right\} \\ &\quad + \left\|P^{-1}(\mathbf{p})\right\| \left\| \frac{\partial \bar{\mathbf{g}}}{\partial \mathbf{x}}(\mathbf{p}) \right\| \|P(\mathbf{p})\| \\ &\quad \text{(by (9))} \\ &\leq \max \left\{ \frac{-(d_i+1)}{b_i} : i = 1, \dots, n \right\} \\ &\quad + \max_{i=1}^n \{d_i\} \cdot \|J_{\bar{\mathbf{g}}}(\bar{\pi}(F_1))\|_2 \cdot \max_{i=1}^n \left\{ \frac{(b_i)^{d_i+1}}{d_i} \right\}. \end{aligned}$$

Q.E.D.

Lemma 12 If $d \geq \bar{d}(F_1)$, we have:

$$(a) \mu_2(J_{\bar{\mathbf{g}}}(\pi(F_1))) \leq (-2 + (\check{b}_{\max})^{d+2}) \cdot \frac{\|J_{\bar{\mathbf{g}}}(\bar{\pi}(F_1))\|_2}{\check{b}_{\max}}.$$

$$(b) \text{ If } \log_2(\check{b}_{\max}) < \frac{1}{d+2} \text{ then } \mu_2(J_{\bar{\mathbf{g}}}(\pi(F_1))) < 0.$$

Proof.

(a) By Theorem 11 we have

$$\begin{aligned} \mu_2(J_{\bar{\mathbf{g}}}(\pi(F_1))) &\leq -(d+1)\frac{1}{\check{b}_{\max}} + (\check{b}_{\max})^{d+1} \|J_{\bar{\mathbf{g}}}(\bar{\pi}(F_1))\|_2 \\ &= \left(\frac{-(d+1)}{\|J_{\bar{\mathbf{g}}}(\bar{\pi}(F_1))\|_2} + (\check{b}_{\max})^{d+2} \right) \cdot \frac{\|J_{\bar{\mathbf{g}}}(\bar{\pi}(F_1))\|_2}{\check{b}_{\max}} \\ &\quad \text{(by factoring)} \\ &\leq \left(-2 + (\check{b}_{\max})^{d+2} \right) \cdot \frac{\|J_{\bar{\mathbf{g}}}(\bar{\pi}(F_1))\|_2}{\check{b}_{\max}} \\ &\quad \text{(By eqn.(34), we have } (d+1) \geq 2(\|J_{\bar{\mathbf{g}}}(\bar{\pi}(F_1))\|_2)). \end{aligned}$$

$$(b) \text{ Since } (\check{b}_{\max})^{d+2} < 2 \text{ is equivalent to } \log_2(\check{b}_{\max}) < \frac{1}{d+2}, \text{ we conclude that } \mu_2(J_{\bar{\mathbf{g}}}(\pi(F_1))) < 0.$$

Q.E.D.

Lemma A.4

Let $\mathbf{p}, \mathbf{q} \in B \subseteq \mathbb{R}^n$ and $\phi \in C^1(F_1 \rightarrow \mathbb{R}^n)$, then $\|\phi(\mathbf{p}) - \phi(\mathbf{q})\|_2 \leq \|J_\phi(B)\|_2 \cdot \|\mathbf{p} - \mathbf{q}\|_2$

Proof.

$$\begin{aligned} \|\phi(\mathbf{p}) - \phi(\mathbf{q})\|_2 &\leq \|\phi(\mathbf{q}) + J_\phi(\xi) \cdot (\mathbf{p} - \mathbf{q}) - \phi(\mathbf{q})\|_2 \\ &\quad \text{(by Taylor expansion of } \phi(\mathbf{p}) \text{ at } \mathbf{q}) \\ &= \|J_\phi(\xi) \cdot (\mathbf{p} - \mathbf{q})\|_2 \\ &\leq \|J_\phi(\xi)\|_2 \cdot \|\mathbf{p} - \mathbf{q}\|_2 \\ &\leq \|J_\phi(B)\|_2 \cdot \|\mathbf{p} - \mathbf{q}\|_2, \end{aligned}$$

where $\xi \in B$.

Q.E.D.

Lemma 13 Let $\mathbf{y} = \pi(\mathbf{x})$ and

$$\begin{aligned} \mathbf{x} &\in \text{IVP}_f(\mathbf{x}_0, h, F_1), \\ \mathbf{y} &\in \text{IVP}_g(\pi(\mathbf{x}_0), h, \pi(F_1)). \end{aligned}$$

For any $\delta > 0$ and any point $\mathbf{p} \in \mathbb{R}^n$ satisfying

$$\|\pi(\mathbf{p}) - \mathbf{y}(h)\|_2 \leq \frac{\delta}{\|J_{\pi^{-1}}(\pi(F_1))\|_2},$$

we have

$$\|\mathbf{p} - \mathbf{x}(h)\|_2 \leq \delta.$$

Proof.

$$\begin{aligned} \|\mathbf{p} - \mathbf{x}(h)\|_2 &= \|\pi^{-1}(\pi(\mathbf{p})) - \pi^{-1}(\pi(\mathbf{x}(h)))\|_2 \\ &= \|\pi^{-1}(\pi(\mathbf{p})) - \pi^{-1}(\mathbf{y}(h))\|_2 \\ &\leq \|J_{\pi^{-1}}(\pi(F_1))\|_2 \cdot \|\pi(\mathbf{p}) - \mathbf{y}(h)\|_2 \\ &\quad \text{(by Lemma A.4)} \\ &\leq \delta \quad \text{(by condition (36).)} \end{aligned}$$

Q.E.D.

Theorem 14 The subroutine *S.Refine*(ϵ) is correct. In particular, it halts.

Proof. The proof is in two parts: (a) partial correctness and (b) termination. Assume the scaffold S has m stages and the input for *Refine* is $\epsilon > 0$.

(a) Partial correctness is relatively easy, so we give sketch a broad sketch: we must show that if the *Refine* halts, then its output is correct, i.e., $w_{\max}(E_m(S)) < \epsilon$. The first line of *Refine* initializes r_0 to $w_{\max}(E_m(S))$. If $r_0 < \epsilon$, then we terminate without entering the while-loop, and the result hold. If we enter the while-loop, then we can only exit the while-loop if the last line of the while-body assigns to r_0 a value $w_{\max}(E_m(S))$ less than ϵ . Again this is correct.

(b) The rest of the proof is to show that *Refine* halts. We will prove termination by way of contradiction. If *Refine* does not terminate, then it has infinitely many **phases** where the k th phase ($k = 1, 2, \dots$) refers to the k iterate of the while-loop.

(H1) We will show that $\lim_{k \rightarrow \infty} \delta_i^k = 0$ for each $i = 1, \dots, m$ in (42). This will yield a contradiction.

(H2) For a fixed stage i , we see the number of times that *Refine* calls *EulerTube* is

$$d_i^k := \log_2 \left(\frac{\delta_i^1}{\delta_i^k} \right).$$

Similarly, the number of times `Refine` calls `Bisect` is

$$\ell_i^k - \ell_i^1$$

where ℓ_i^k is the level of the (k, i) phase-stage. So,

$$k = d_i^k + (\ell_i^k - \ell_i^1) \quad (58)$$

since each phase calls either `Bisect` or `EulerTube`. Hence $k \rightarrow \infty$.

(H3) **CLAIM:** $\lim_{k \rightarrow \infty} d_i^k \rightarrow \infty$, i.e., `EulerTube` is called infinitely often. By way of contradiction, suppose d_i^k has an upper bound, say \bar{d}_i^k . Since μ_2 , Δt_i , and \bar{M} are bounded, we have $\hat{h} \geq C \cdot 2^{\bar{d}_i^k}$ in `Refine` (see (12)), where $C > 0$ is a constant.

Note that each `Bisect(i)` increments the level and thus halves H . Therefore, once $H < C \cdot 2^{\bar{d}_i^k}$, `Bisect` will no longer be called. This implies that $\lim_{k \rightarrow \infty} (\ell_i^k - \ell_i^1)$ is finite. This contradicts the fact that $k \rightarrow \infty$ since both d_i^k and $(\ell_i^k - \ell_i^1)$ are bounded. Thus, our **CLAIM** is proved.

It follows from the **CLAIM** that $\lim_{k \rightarrow \infty} \delta_i^k = 0$, since `EulerTube` is called infinitely often, and after each call, δ_i^k is halved.

(H4) Consider (k, i) as a **phase-stage**: define r_i^k as the radius of the circumball of $E_i(S)$ at phase k . For instance, we terminate in phase k if $k \geq 0$ is the first phase to satisfy $r_m^k < \frac{1}{2}\varepsilon_0$.

Since we call `EulerTube` infinitely often, and each call ensures that the target δ_i^k is reached by r_i^k in the sense of satisfying the inequality

$$r_i^k \leq r_{i-1}^k e^{\mu_i^k \Delta t_i} + \delta_i^k, \quad (59)$$

where μ_i^k (computed as μ_2 in `Refine`) is an upper bound for the logarithmic norm over the full enclosure of the i th stage.

(H5) A **chain** is a sequence $C_1 = (1 \leq k(1) \leq k(2) \leq \dots \leq k(m))$ such that `EulerTube` is called in phase-stage $(k(i), i)$ for each $i = 1, \dots, m$. The chain contains m inequalities of the form (59), and we can telescope them into a single inequality.

But first, to simplify these inequalities, let $\bar{\mu}$ be the largest value of μ_i^1 for $i = 1, \dots, m$, $\Delta = \Delta(C_1)$ is $\max_{i=1}^k \delta_i^{k(1)}$, and h_i be the step size of the i th stage:

$$\begin{aligned} r_m^{k(m)} &\leq (r_{m-1}^{k(m)}) e^{\mu_i^{k(m)} h_i} + \delta_i^{k(m)} && \text{(by (59) for } (k(m), m)) \\ &\leq (r_{m-1}^{k(m-1)}) e^{\mu_i^{k(m)} h_i} + \delta_i^{k(m)} && \text{(since } r_{m-1}^{k(m)} \leq r_{m-1}^{k(m-1)}) \\ &\leq ((r_{m-2}^{k(m-1)}) e^{\mu_{i-1}^{k(m-1)} h_{i-1}} + \delta_{i-1}^{k(m-1)}) e^{\mu_i^{k(m)} h_i} + \delta_i^{k(m)} && \text{(by (59) for } (k(m-1), m-1)) \\ &\leq ((r_{m-2}^{k(m-1)}) e^{\bar{\mu} h_{i-1}} + \Delta) e^{\bar{\mu} h_i} + \Delta && \text{(simplify using } \bar{\mu}, h_i, \Delta) \\ &\vdots \\ &\leq (r_0^{k(1)}) e^{\bar{\mu} \sum_{j=1}^m h_j} + \Delta \cdot \left(\sum_{j=0}^{m-1} e^{\bar{\mu} \sum_{i=j+1}^m h_i} \right) \\ &\leq e^{\bar{\mu}} (r_0^{k(1)} + \Delta \cdot m) && \text{(since } 1 \geq \sum_{i=1}^m h_i) \end{aligned}$$

To summarize what we just proved¹³ about a chain C_1 , let $r_m(C_1)$ denote $r_m^{k(m)}$ and $r_0(C_1)$ denote $r_0^{k(1)}$ the following **C_1 -inequality**:

$$r_m(C_1) \leq e^{\bar{\mu}} (r_0(C_1) + \Delta(C_1) \cdot m). \quad (60)$$

¹³This proof assumes that $\mu_i^k \leq \mu_i^{k-1}$. This is true if our interval computation of μ_2 is isotonic. But we can avoid assuming isotony by defining μ_i^k to be μ_i^{k-1} if the computation returns a larger value.

(H6) If $C = (1 \leq k(1) \leq \dots \leq k(m))$ and $C' = (1 \leq k'(1) \leq \dots \leq k'(m))$ are two chains where $k(i) < k'(i)$ for $i = 1, \dots, m$, then we write $C < C'$.

LEMMA H6: If $C < C'$ then

$$r_m(C') \leq \frac{1}{2} e^{\bar{\mu}} (r_0(C) + \Delta(C) \cdot m)$$

(H7) It is easy to show that there exists an infinite sequence of chains

$$C_1 < C_2 < C_3 < \dots$$

This comes from the fact that for each $i = 1, \dots, m$, there are infinitely many phases that calls EulerTube. It follows by induction using the previous LEMMA H6 that, for each $i \geq 2$,

$$r_m(C_i) \leq \left(\frac{1}{2}\right)^i e^{\bar{\mu}} (r_0(C_1) + \Delta(C_1) \cdot m)$$

This proves that $\lim_{i \rightarrow \infty} r_m(C_i) = 0$. This contradicts the non-termination of Refine.

Q.E.D.

Theorem 15 *Algorithm EndEnc(B_0, ε_0) halts, provided the interval computation of StepA is isotonic. The output is also correct.*

Proof.

If the algorithm terminates, its correctness is ensured by the conclusions in Section 4.

We now proceed to prove the termination of the algorithm. Specifically, we need to show that the loop in the algorithm can terminate, which means that the time variable t can reach 1. It suffices to demonstrate that for any inputs B_0 and $\varepsilon_0 > 0$, there exists a lower bound $\underline{h} > 0$ such that for the i th iteration of the loop has step size $\Delta t_i = h_i \geq \underline{h}$.

First we define the set $\bar{E} := \text{image}(\text{IVP}(B_0, 1)) + [-\varepsilon_0, \varepsilon_0]^n$. Since $\text{IVP}(B_0, 1)$ is valid, \bar{E} is a bounded set. Let the pair (\underline{h}, \bar{F}) be the result of calling the subroutine $\text{StepA}(\bar{E}, 1, \varepsilon_0)$. Note that StepA is implicitly calling box functions to compute \underline{h}, \bar{F} (see Subsection 2.2), and thus \underline{h} is positive. Whenever we call StepA in our algorithm, its arguments are (E, H, ε_0) for some $E \subseteq \bar{E}$ and $H \leq 1$. If $\text{StepA}(E, H, \varepsilon_0) \rightarrow (h, F)$, then $h \geq \underline{h}$, provided¹⁴ StepA is isotonic. This proves that the algorithm halts in at most $\lceil 1/\underline{h} \rceil$ steps. **Q.E.D.**

B. Appendix B: The affine map $\bar{\pi}$

Consider the condition (30). Without loss of generality, assume $0 \notin \bar{I}_1$. To further simplify our notations, we assume

$$\bar{I}_1 > 0. \tag{61}$$

In case $\bar{I}_1 < 0$, we shall indicate the necessary changes to the formulas. We first describe an invertible linear map $\tilde{\pi} : \mathbb{R}^n \rightarrow \mathbb{R}^n$ such that

$$\tilde{\pi}(f(B_1)) > \mathbf{1} = (1, \dots, 1) \quad (\text{Greater-than-One Property of } \tilde{\pi}) \tag{62}$$

Note that (62) means that for each $i = 1, \dots, n$, the i th component $(\tilde{\pi}(f(B_1)))_i$ is greater than one.

To define $\tilde{\pi}$, we first introduce the box \tilde{B}_1 :

$$\begin{aligned} \tilde{B}_1 & := \text{Box}(f(B_1)) \\ & = \prod_{i=1}^n \bar{I}_i \quad (\text{implicit definition of } \bar{I}_i) \\ & = \prod_{i=1}^n [\bar{a}_i, \bar{b}_i] \quad (\text{implicit definition of } \bar{a}_i, \bar{b}_i) \end{aligned} \tag{63}$$

¹⁴If computes $h > \underline{h}$, we could not “simply” set h to be \underline{h} because we do not know how to compute a corresponding full enclosure. Note that \bar{E} is a full enclosure, but we do not know how to compute it.

where $\text{Box}(S) \in \square \mathbb{R}^n$ is the smallest box containing a set $S \subseteq \mathbb{R}^n$. For instance, $\bar{I}_i = f_i(B_1)$ where $\mathbf{f} = (f_1, \dots, f_n)$. The assumption (61) says that $\bar{I}_1 > 0$, i.e., either $\bar{a}_1 > 0$.

We now define the map $\tilde{\pi} : \mathbb{R}^n \rightarrow \mathbb{R}^n$ as follows: $\tilde{\pi}(x_1, \dots, x_n) = (\tilde{x}_1, \dots, \tilde{x}_n)$ where

$$\tilde{x}_i := \begin{cases} \frac{x_i}{\bar{a}_i} & \text{if } \bar{a}_i > 0, \quad (\text{i.e., } f_i(B_1) > 0) \\ \frac{x_i}{\bar{b}_i} & \text{else if } \bar{b}_i < 0, \quad (\text{i.e., } f_i(B_1) < 0) \\ x_i + x_1 \left(\frac{1 + \bar{b}_i - \bar{a}_i}{\bar{a}_1} \right) & \text{else} \quad (\text{i.e., } 0 \in f_i(B_1)). \end{cases} \quad (64)$$

Note that if $\bar{I}_1 < 0$, we only need to modify the third clause in (64) to $x_i + x_1 \left(\frac{1 + \bar{b}_i - \bar{a}_i}{\bar{b}_1} \right)$.

Observe that $\tilde{\pi}(\tilde{B}_1)$ is generally a parallelepiped, not a box. Even for $n = 2$, $\tilde{\pi}(\tilde{B}_1)$ is a parallelogram. So we are interested in the box $\text{Box}(\tilde{\pi}(\tilde{B}_1))$:

$$\begin{aligned} B'_1 := \text{Box}(\tilde{\pi}(\tilde{B}_1)) &= \prod_{i=1}^n I'_i \quad (\text{implicit definition of } I'_i) \\ &= \prod_{i=1}^n [a'_i, b'_i] \quad (\text{implicit definition of } a'_i, b'_i) \end{aligned} \quad (65)$$

Then we have the following results:

Lemma B.1

(a) $\tilde{\pi}$ is an invertible linear map given by

$$\tilde{\pi}(\mathbf{x}) = \bar{A} \bullet \mathbf{x} \quad (66)$$

and the matrix \bar{A} has the structure:

$$\begin{bmatrix} v_1 & & & & & \\ c_2 & v_2 & & & & \\ c_3 & & v_3 & & & \\ \vdots & & & \ddots & & \\ c_n & & & & & v_n \end{bmatrix}$$

where

$$v_i = \begin{cases} \frac{1}{\bar{a}_i} & \text{if } \bar{a}_i > 0, \\ \frac{1}{\bar{b}_i} & \text{else if } \bar{b}_i < 0, \\ 1 & \text{else} \end{cases}$$

$$c_i = \begin{cases} 0 & \text{if } 0 \notin f_i(B_1), \\ \frac{1 + \bar{b}_i - \bar{a}_i}{\bar{a}_1} & \text{else.} \end{cases}$$

(b) The box $\text{Box}(\tilde{\pi}(\tilde{B}_1)) = \prod_{i=1}^n I'_i$ is explicitly given by

$$I'_i = \begin{cases} \left[1, \frac{\bar{b}_i}{\bar{a}_i} \right] & \text{if } \bar{a}_i > 0, \\ \left[1, \frac{\bar{a}_i}{\bar{b}_i} \right] & \text{else if } \bar{b}_i < 0, \\ \left[1 + \bar{b}_i, \frac{\bar{b}_1}{\bar{a}_1} \left(1 + \bar{b}_i \left(1 + \frac{\bar{a}_1}{\bar{b}_1} \right) - \bar{a}_i \right) \right] & \text{else.} \end{cases} \quad (67)$$

(c) The map $\tilde{\pi}$ has the positivity property of (62).

Proof.

(a) From the definition of $\tilde{\pi}$ in (64), we see that the matrix \bar{A} matrix the form described in the lemma. This matrix is clearly invertible.

(b) We derive explicit formulas for I'_i in each of the 3 cases:

- If $\bar{a}_i > 0$, then it is clear that $(\tilde{\pi}(B_1))_i = \left[1, \frac{\bar{b}_i}{\bar{a}_i}\right]$.
- Else if $\bar{b}_i < 0$, it is also clear that $(\tilde{\pi}(B_1))_i = \left[1, \frac{\bar{a}_i}{\bar{b}_i}\right]$.
- Else, we consider an arbitrary point $\mathbf{x} = (x_1, \dots, x_n) \in \tilde{B}_1$:

$$\begin{aligned}
(\tilde{\pi}(\mathbf{x}))_i &= x_i + x_1 \left(\frac{1+\bar{b}_i-\bar{a}_i}{\bar{a}_1}\right) && \text{(by definition)} \\
&\geq \bar{a}_i + \bar{a}_1 \left(\frac{1+\bar{b}_i-\bar{a}_i}{\bar{a}_1}\right) \\
&\quad (x_j \in [\bar{a}_j, \bar{b}_j] (\forall j) \ \&\ (1 + \bar{b}_i - \bar{a}_i)/\bar{a}_1 > 0) \\
&= 1 + \bar{b}_i. \\
(\tilde{\pi}(\mathbf{x}))_i &= x_i + x_1 \left(\frac{1+\bar{b}_i-\bar{a}_i}{\bar{a}_1}\right) \\
&\leq \bar{b}_i + \bar{b}_1 \left(\frac{1+\bar{b}_i-\bar{a}_i}{\bar{a}_1}\right) \\
&\quad (x_j \in [\bar{a}_j, \bar{b}_j] \text{ and } (1 + \bar{b}_i - \bar{a}_i)/\bar{a}_1 > 0) \\
&= \frac{\bar{b}_1}{\bar{a}_1} \left(1 + \bar{b}_i \left(1 + \frac{\bar{a}_1}{\bar{b}_1}\right) - \bar{a}_i\right).
\end{aligned}$$

Since both the upper and lower bounds are attainable, they determine the interval I'_i as claimed.

(c) It is sufficient to show that $I'_i \geq 1$. This is clearly true for the first two clauses of (67). For the last two clauses, we have $I'_i \geq 1 + \bar{b}_i$ by part(b). The result follows since $0 \leq \bar{b}_i$.

Q.E.D.

Let

$$\begin{aligned}
B_1^* &:= \text{Box}(\tilde{\pi}(B_1)) \\
&= \prod_{i=1}^n I_i^* \quad (\text{implicit definition of } I_i^*) \\
&= \prod_{i=1}^n [a_i^*, b_i^*] \quad (\text{implicit definition of } a_i^*, b_i^*)
\end{aligned} \tag{68}$$

We now define the affine map $\bar{\pi} : \mathbb{R}^n \rightarrow \mathbb{R}^n$:

$$\begin{aligned}
\bar{\pi}(\mathbf{x}) &= (\bar{\pi}_1(x_1), \bar{\pi}_2(x_2), \dots, \bar{\pi}_n(x_n)) \\
&\quad \text{where } \mathbf{x} = (x_1, \dots, x_n) \text{ and} \\
\bar{\pi}_i(x) &:= \tilde{\pi}(x) - a_i^* + 1.
\end{aligned} \tag{69}$$

Then we have the following results, which is property (Q2):

Lemma B.2 $\bar{\pi}(B_1) > \mathbf{1}$.

Proof. The conclusion follows from the fact that $\tilde{\pi}(B_1) \subseteq \prod_{i=1}^n [a_i^*, b_i^*]$ and $\bar{\pi}(B_1) = \tilde{\pi}(B_1) - (a_1^*, \dots, a_n^*) + \mathbf{1}$.

Q.E.D.

References

- [1] E. Adams, D. Cordes, and R. Lohner. Enclosure of solutions of ordinary initial value problems and applications. In E. Adams, R. Ansorge, C. Großmann, and H. Roos, editors, *Discretization in Differential Equations and Enclosures*, pages 9–28. Akademie-Verlag, Berlin, 1987.
- [2] O. Bournez, D. S. Graça, and A. Pouly. Solving analytic differential equations in polynomial time over unbounded domains. In *MFCS'11: Proc. 36th Int'l Conf. Math. Foundations of Computer Sci.*, Berlin, Heidelberg, 2011. Springer-Verlag.
- [3] F. Bünger. A Taylor Model Toolbox for solving ODEs implemented in MATLAB/INTLAB. *J. Comp. and Appl. Math.*, 368:112511, 2020.
- [4] F. Bünger. Preconditioning of Taylor models, implementation and test cases. *Nonlinear Theory and its Applications, IEICE*, 12(1):2–40, 2021.
- [5] Computer assisted proofs in dynamics group, 2025. URL <http://capd.ii.uj.edu.pl/>.
- [6] Core Library Homepage, since 1999. Software download, source, documentation and links: https://cs.nyu.edu/exact/core_pages/svn-core.html.
- [7] G. F. Corliss. Survey of interval algorithms for ordinary differential equations. *Appl.Math.Comp.*, 31, 1989.
- [8] G. F. Corliss and R. Rihm. Validating an a priori enclosure using high-order Taylor series. In G. Alefeld and A. Frommer, editors, *Scientific Computing, Computer Arithmetic, and Validated Numerics*, Elsevier Studies in Computational Mathematics, pages 228–238. Akademie Verlag, Berlin, 1996.
- [9] C. Desoer and H. Haneda. The measure of a matrix as a tool to analyze computer algorithms for circuit analysis. *IEEE Trans. on Circuit Theory*, 19(5):480–486, 1972.
- [10] P. Eijgenraam. The solution of initial value problems using interval arithmetic: formulation and analysis of an algorithm. *Mathematical Centre Tracts*, No. 144, 1981.
- [11] C. Fan, J. Kapinski, X. Jin, and S. Mitra. Simulation-driven reachability using matrix measures. *ACM Trans. on Embedded Computing Systems*, 17(1):21:1–28, 2018. Special Issue on Autonomous Battery-Free Sensing and Communication.
- [12] O. Goldreich. On Promise Problems (a survey). In *Theoretical Computer Science: Essays in memory of Shimon Even*, pages 254 – 290. Springer, 2006. LNCS. Vol. 3895.
- [13] D. Graça, N. Zhong, and J. Buescu. Computability, noncomputability and undecidability of maximal intervals of IVPs. *Trans. AMS*, 361(6):2913–2927, 2009.
- [14] E. Hairer, S. P. Nørsett, and G. Wanner. *Solving Ordinary Differential Equations I: Nonstiff Problems*. Springer-Verlag, Berlin, second revised edition, 2008.
- [15] K. Hormann, L. Kania, and C. Yap. Novel range functions via taylor expansions and recursive lagrange interpolation with application to real root isolation. In *Int'l Symp. Symbolic and Alge. Comp.(46th ISSAC)*, pages 193–200, New York, 2021. ACM Press. July 18–23. St. Petersburg, Russia. Software download from https://cs.nyu.edu/exact/core_pages/svn-core.html.
- [16] K. Hormann, C. Yap, and Y. A. Zhang. Range functions of any convergence order and their amortized complexity analysis. In *Computer Algebra in Scientific Computing (25th CASC)*, volume 14139 of LNCS, pages 162–182. Springer, 2023. Aug 28 - Sep 1, University of Havana, Cuba. <http://www.casc-conference.org/>. Software download from https://cs.nyu.edu/exact/core_pages/svn-core.html.
- [17] K. Jackson and N. S. Nedialkov. Some recent advances in validated methods for ivps for odes. *Applied Numerical Mathematics*, 42:269–284, 2002.
- [18] T. Kapela, M. Mrozek, D. Wilczak, and P. Zgliczyński. CAPD::DynSys: a flexible C++ toolbox for rigorous numerical analysis of dynamical systems. *Communications in Nonlinear Sci. and Numerical Simulation*, 101:105578, 2021.
- [19] K.-I. Ko. *Complexity Theory of Real Functions*. Progress in Theoretical Computer Science. Birkhäuser, Boston, 1991.
- [20] R. Lohner. *Einschließung der Lösung gewöhnlicher Anfangs – und Randwertaufgaben und Anwendungen*. Phd thesis, Universität Karlsruhe, 1988.
- [21] K. Makino and M. Berz. Verified computations using taylor models and their applications. In *LNCS No. 10381*, pages 3–13, 2017.
- [22] R. Moore. Interval Analysis: Differential Equations. In C. A. Floudas and P. M. Pardalos, editors, *Encyclopedia of Optimization*, pages 1686–1689. Springer, 2nd edition, 2009.
- [23] R. E. Moore. The automatic analysis and control of error in digital computation based on the use of interval numbers. In L. B. Rall, editor, *Error in digital computation, Volume 1*, pages 61–130. Wiley New York, 1965. Proc. of an Advanced Seminar conducted by the Mathematics Research Center, United States Army, University of Wisconsin, Madison, October 5-7, 1964.
- [24] R. E. Moore. *Interval Analysis*. Prentice Hall, Englewood Cliffs, NJ, 1966.
- [25] N. S. Nedialkov. *Computing Rigorous Bounds on the Solution of an Initial Value Problem for an Ordinary Differential Equation*. PhD thesis, Department of Computer Science, University of Toronto, 1999.
- [26] N. S. Nedialkov, K. R. Jackson, , and J. D. Pryce. An effective high-order interval method for validating existence and uniqueness of the solution of an IVP for an ODE. *Reliable Computing*, 7(6):449–465, 2001.
- [27] N. S. Nedialkov, K. R. Jackson, and G. F. Corliss. Validated solutions of initial value problems for ordinary differential equations. *Applied Mathematics and Computation*, 105(1):21–68, 1999.
- [28] A. Neumaier. Global, rigorous, and realistic bounds for the solution of dissipative differential equations. Part I: Theory. *Computing*, 52:315–336, 1994.
- [29] K. Nickel. How to fight the wrapping effect. In *Proc. Intl Symp. on Interval mathematics*, pages 121–132, Berlin, 1986. Springer-Verlag.
- [30] C. V. Pao. Logarithmic derivatives of a square matrix. *Linear Algebra and its Appl.*, 6:159–164, 1973.
- [31] N. Revol. Affine iterations and wrapping effect: Various approaches, 2022.
- [32] R. Rihm. Interval methods for initial value problems in odes. In J. Herzberger, editor, *Topics in validated computations: Proc. of the IMACS-GAMM Int'l Workshop on Validated Computations*, Elsevier Studies in Computational Mathematics, pages 173–207. Elsevier, 1994.
- [33] J. K. Scott and P. L. Barton. Bounds on the reachable sets of nonlinear control systems. *Automatica*, 49:93–100, 2013.

- [34] K. Shen, D. L. Robertson, and J. K. Scott. Tight reachability bounds for constrained nonlinear systems using mean value differential inequalities. *Automatica*, 134:109911, 2021.
- [35] G. Söderlind. The logarithmic norm. history and modern theory. *BIT Numerical Mathematics*, 46(3):631–652, 2006.
- [36] A. J. Sommese, J. Verschelde, and C. W. Wampler. Introduction to numerical algebraic geometry. In A. Dickenstein and I. Z. Emiris, editors, *Solving Polynomial Equations: Foundations, Algorithms, and Applications*. Springer, 2010.
- [37] H. J. Stetter. Validated solution of initial value problems for ODE. In C. Ullrich, editor, *Computer Arithmetic and Self-Validating Numerical Methods*, volume 7 of *Notes and Reports in Mathematics, Science and Engineering*, pages 171–187. Academic Press, 1990.
- [38] T. Strom. On logarithmic norms. *SIAM Journal on Numerical Analysis*, 12(5):741–753, 1975.
- [39] I. Walawska and D. Wilczak. An implicit algorithm for validated enclosures of the solutions to the variational equations for ODEs. *Applied Mathematics and Computation*, 291:303–322, 2016.
- [40] D. Wilczak and P. Zgliczynski. C^r -Lohner algorithm. *Schedae Informaticae*, 20:9–42, 2011.
- [41] J. Xu, M. Burr, and C. Yap. An approach for certifying homotopy continuation paths: Univariate case. In *Int'l Symp. Symbolic and Alge. Comp.*, pages 399–406, 2018. 43rd ISSAC. July 16-19. New York City.
- [42] J. Xu and C. Yap. Effective subdivision algorithm for isolating zeros of real systems of equations, with complexity analysis. In *Int'l Symp. Symbolic and Alge. Comp.(44th ISSAC)*, pages 355–362, New York, 2019. ACM Press. July 15-18. Beijing.
- [43] J. Yu, C. Yap, Z. Du, S. Pion, and H. Bronnimann. Core 2: A library for Exact Numeric Computation in Geometry and Algebra. In *3rd Proc. Int'l Congress on Mathematical Software (ICMS)*, pages 121–141, Heidelberg, 2010. Springer. Kobe, Japan. Sep 13-17, 2010. LNCS No. 6327.
- [44] P. Zgliczynski. C^1 -Lohner algorithm. *Foundations of Computational Mathematics*, 2(4):429–465, 2002.